

EXPERIMENTAL AND THEORETICAL INVESTIGATIONS CONCERNING A "FREQUENCY
FILTER BEHAVIOR" OF THE HUMAN RETINA REGARDING ELECTRIC
PULSE CURRENTS

A. Meier-Koll

Translation of "Experimentelle und theoretische Untersuchungen über ein Fre-
quenzfilterverhalten der menschlichen Retina gegenüber elektrischen Im-
pulsströmen," Munich, West Germany, Technische Hochschule, Fakul-
tät für Maschinenwesen und Elektrotechnik, Doctoral disserta-
tion in Engineering, 1970, 90 pages.

1. Report No. NASA TM-75372	2. Government Accession No.	3. Recipient's Catalog No.	
4. Title and Subtitle EXPERIMENTAL AND THEORETICAL INVESTIGATIONS CONCERNING A "FREQUENCY FILTER BEHAVIOR" OF THE HUMAN RETINA REGARDING ELECTRIC PULSE CURRENTS		5. Report Date September 1979	
		6. Performing Organization Code	
7. Author(s) A: Meier-Koll		8. Performing Organization Report No.	
		10. Work Unit No.	
9. Performing Organization Name and Address Leo Kanner Associates Redwood City, California 94063		11. Contract or Grant No. NASw-3199	
		13. Type of Report and Period Covered Translation	
12. Sponsoring Agency Name and Address National Aeronautics and Space Administration Washington, D.C. 20546		14. Sponsoring Agency Code	
		15. Supplementary Notes Translation of "Experimentelle und theoretische Untersuchungen über ein Frequenzfilterverhalten der menschlichen Retina gegenüber elektrischen Impulsströmen", Munich, West Germany, Technische Hochschule, Fakultät für Maschinenwesen und Elektrotechnik, Doctoral dissertation in Engineering, 1970, 90 p. (A71-14372)	
16. Abstract Discussion of investigations involving patients with injuries in the visual nervous system, which lead to an identification of the epithelial ganglion of the retina as a frequency filter taking also into consideration a model of the retinal ganglion which can account for the observed behavior. Threshold curves of the injured visual organs are compared with threshold curves obtained with a control group as a basis for identification. A model which considers the epithelial ganglion as a homogeneous cell layer in which adjacent neurons interact is discussed. It is shown how the behavior of the cells against alternating exciting currents can be explained.			
17. Key Words (Selected by Author(s))		18. Distribution Statement Unclassified-Unlimited	
19. Security Classif. (of this report) Unclassified	20. Security Classif. (of this page) Unclassified	21. No. of Pages 58	22. Price

Summary

Even inadequate excitation of the human eye with low frequency electric pulse currents has the power to create impressions of light. In earlier works of the Japanese authors Motokawa and Abe it was shown, that the excitation threshold of such light perceptions is a function of the series frequency of the electric excitation pulses. This frequency dependence is expressed by the fact, that local minima are attached to the excitation threshold of light perception for specific frequencies. It is true that the authors reported somewhat different values for these preferred frequencies, yet taken together their frequency values are whole multiples of a basic frequency that lies around 10 Hz. On the strength of such a finding we may assume that in the visual nervous system there exists a nerve center which functions as a harmonious frequency filter in respect to the pulse currents. Since there is a difference in threshold minima in their strength at changing levels of adaptation, the authors cited above believed that the filter behavior should be attributed to the retinal photoreceptors. However they were not able to arrive at conclusive proof about the seat of the filter mechanism.

The experimental investigations of the present dissertation applied to the selection of that frequency filter. Inasmuch as injury to the nerve center in question must destroy the frequency filter property, it ought to be possible to determine the seat of such a frequency filter through threshold measurements done on patients exhibiting selective lesions of the visual nervous system. Using this concept we reported threshold curves for damaged visual organs in patients at the University of Munich Eye Clinic and compared them with the threshold curves of a control group. On the basis of these measurements we were able to identify the ganglion epithelium of the retina.

For the interpretation of frequency filter behavior toward alternating excitation currents the theoretical portion of the dissertation develops a system model of the retinal ganglion epithelium. Drawing on known histological studies of the retina, this theory conceives the ganglion epithelium as a homogeneous layer of cells in which adjacent nerve cells (neurons) may exhibit neural interplay. Exciting and inhibiting exchanges between different neurons were conceived in such a way, that any excitation of a ganglion cell spread like a ripple to the rest of the epithelium. If we expose this hypothetical assemblage of neurons to an alternating excitation current, these ripples are released by each ganglion in the rhythm of the excitation frequency. The ripples may then provide constructive or destructive interference. As the theory shows, the result of constructive interference are excitation conditions in the total ganglion epithelium, whenever the excitation frequency amounts approximately to a whole multiple of the basic frequency. In such cases it is only necessary for the excitation strength to be small to produce in the retinal ganglia an excitation level which corresponds to the threshold value for light perception. This comprises the theoretical interpretation of the frequency filter behavior.

The proposed model has likewise a "biological meaning". Projection of a moving luminous point onto the retina applies a succession of stimulation points to various ganglion cells along its path. In the process the excitation waves released by these neurons interfere in the form of a shock wave, which hurries ahead of the excitation point and preactivates precisely those

ganglia which the excitation point will sweep over in the next instant. In the final analysis such a "forewarning" reduces the information that the brain has to process in the apperception of the moving point of light. Thus the theory attributes to the retinal ganglion epithelium the role of "motion analyzer". This same "motion analyzer", when exposed to the artificial alternating currents, exhibits properties of a frequency filter.

Finally, the theoretic system model helps create the possibility of using pictures of threshold curves for distinguishing total and partial injuries to various layers of the retina. Such a procedure for the differential diagnosis of retinal lesions would be useful for example in cataract diseases where optic examination of the fundus is out of the question.

I will always remember gratefully my deceased doctoral supervisor, Prof. Dr. M. Knoll, for his untiring support of my work.

I am very grateful to Dr. J. Eichmeier, Lecturer, for his eager support of my candidacy and for proofreading the manuscript.

I am much indebted to Dr. O.E. Lund, Director of the Eye Clinic of the University of Munich, for permission to carry on my experimental research.

My special thanks to the Assistant Medical Director, Dr. B. v. Barsewisch, who contributed substantially to the success of the work through his revealing discussions and ophthalmological counsel.

I thank my mother most heartily for producing the faircopy of the dissertation.

TO MY BELOVED PARENTS IN GRATITUDE

Table of Contents

	Page
I Introduction	1
II Definition of the Problem	2
III Experimental investigations of retinal frequency filter behavior in respect to electric pulse currents	3
1. Methods	3
2. Results	4
2.1. Frequency dependence of flicker threshold for test subjects of one control group	4
2.2. Frequency dependence of flicker threshold for test subjects with pathological changes of the retina	7
2.2.1. Injuries to the receptor epithelium	9
a) Total damage to receptor epithelium	9
b) Damage to the central regions of the receptor epithelium	18
c) Functional disconnection of half the receptor epithelium	19
2.2.2. Damage to the central neural retina layers and optic nerve	20
a) Total impairment of central neural retinal layers (bipolar and ganglion epithelium)	21
b) Impairment of central regions of the bipolar and ganglion layer	21
c) Loss of central visual field due to neuritic impairment of the optic fibers	21
2.3. Loss of visual field due to cerebral processes	22
3. Discussion of experimental investigations	22
IV. Theoretical interpretation of the retinal frequency filter property in respect to alternating electric currents using a system model of the ganglion layer	24
1. Definition of the problem	24
2. Mathematical system model of the retinal ganglion epithelium	25
3. Consequences of the theory	29
3.1. Rest activity of the ganglion cells	29
3.2. Reproduction of excitation within the ganglion epithelium	30
3.3. Informational theory aspect of the system model	33
3.4. Spike histograms of the ganglion cells with allowance for temporal excitation gradients	34
3.5. Transfer characteristic of ganglion epithelium in respect to alternating current excitation	34
3.5.1. The non-damped system	37
a) Discrete excitation frequencies	38
b) Average intensity of the excitation pattern	39
3.5.2. The damped system	40
3.6. Theoretical interpretation of the flicker threshold process	42
a) Harmonious minimum frequencies	42
b) Tendential course of the flicker threshold	43
c) The threshold curve	44
3.7. Effect of pathological changes in the retina on the course of the flicker threshold	46
a) Injury to global receptor epithelium	47
b) Injury to central areas of receptor epithelium	47
c) Injury to global ganglion epithelium	48
d) Injury to central areas of ganglion epithelium	48
Bibliography	52

I. Introduction

/1*

As is well known, even inadequate excitation of the human visual organ by low frequency series of electric current pulses may provoke light phenomena. However the stimulation of such flickering light perception, occurring chiefly in the rhythm of the pulse sequence (flicker phosphenes) seems bound by the condition, that at least one of the electrodes is applied in the immediate vicinity of one eye. Thus we may look upon the retina as the primary site of engagement of the electric stimuli.

Various authors (Motokawa and Iwama [9], Abe [1]) have shown by taking the flicker phosphene mentioned above as the index for electric excitability of the visual organ, that the excitation threshold is a function of the series frequency of the electric excitation pulses. This frequency dependence of the excitation threshold was presented by the authors cited in the form of excitation strength-frequency diagrams, where for numerous test frequencies they plotted those tension values which were precisely able to excite the flicker phosphene.

Motokawa and Iwama plotted each time a threshold curve of the dark adapted eye for sinusoidal alternating current and sequences of rectilinear pulses. In both threshold curves local minima appear at 18, 36 and 54 Hz. This drop-off of the excitation threshold for pulse sequences that stand in a numerical harmonious relationship to one another (1:2:3) led Motokawa to conjecture, that the threshold decrements described owed their origin to a resonance mechanism with its seat presumably in some neural tissue of the visual nervous system.

Further measurements by Abe [1] confirmed the investigations of Motokawa for the condition of light adaptation but produced less clear results when extended to the dark adapted eye. The rectangular pulses used by Abe produced threshold curves that passed through local minima at frequencies of 7, 42, 65 and 75 Hz. There is no harmonious numerical relation between these frequencies.

If we arrange the frequency values of all threshold minima according to their amplitude and plot them in a coordinate system against the first integers, we are able to draw a straight line through the points obtained and the point of origin of the coordinate system as shown in Fig. 1. This means, that the frequency values for threshold minima measured under varying conditions of adaptation may still be approximately represented as whole multiples of a basic frequency. /2

* Numbers in the margin indicate pagination in the foreign text

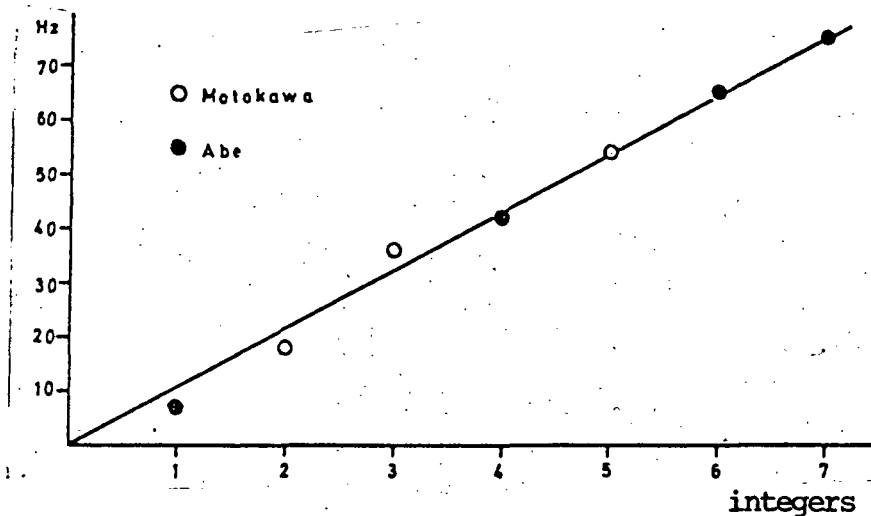


Fig. 1. Evidence of harmonious relationship between minimum frequencies (measured by Motokawa and Abe)

This sort of regularity is reminiscent of resonance mechanism. Due to an inherent resonance mechanism the visual organ might be able to function as a frequency filter which processes preferentially specific frequencies for subjective light sensations.

We would then have to assume, that the retinal photoreceptors influenced the supposed resonance mechanism by bringing out, from the ensemble of all possible threshold minima, various groups at various levels of adaptation. /3

The investigations of the authors mentioned above and the resulting concept of a frequency filter behavior determined by resonance mechanism were the occasion for the present work, whose methodological specification is contained in the statement of the problem which follows.

II. Definition of the Problem

The work is divided into experimental and theoretical investigations concerning the frequency filter behavior of the visual organ.

The experimental questions fall into two groups:

1. Flicker threshold measurements were to be made on a number of test subjects having an intact visual nervous system (control group) so as to discover all possible threshold minima in the interval between zero and 50 Hz. In line with this stipulation measurements were not taken under conditions of light adaptation nor of extreme dark adaptation but at average adaptation levels, such as might occur at minutes 5 and 20 following the beginning of dark adaptation. Thus the intervals between test frequencies would be kept proportionately narrow.

A comparison of results obtained with a number of test subjects would

give an idea of supraindividual fluctuation intervals for corresponding frequency values.

The identical subjects were given a second series of tests some months later to test the reproducibility of frequency dependent threshold behavior over longer time intervals. At the same time such replica measurements permitted us to draw conclusions in respect to the individual amounts of variation in the measurement values. (minimum frequencies).

2. None of the previous works could give an answer as to which portion of the visual organ might be responsible for the observed frequency filter behavior. By extending flicker threshold measurements to patients with pathological changes in specified portions of the visual nervous system we would attempt to discover which neural apparatus acts as a harmonious frequency filter in respect to electric pulse currents. /4

In the theoretical portion of this work the functional relationships which would come to light from the experimental investigations are interpreted by means of a mathematical system model of the nerve structure being studied. A specific definition of the problem for the theoretical investigations presupposes knowledge of the experimental findings and will therefore be appended at the appropriate place.

III. Experimental Investigations of Retinal Frequency Filter Behavior in respect to Electric Pulse Currents

1. Methods

While measurements were being taken the test subjects lay on a couch. Both eyes were shielded by a pair of sleeping glasses. The testing area was darkened. A freshly moistened rag attached to a flannel covered silver electrode (2x2cm) was shoved under the glasses in such a way that the rag lay upon one of the closed eyes. The other electrode could be attached to the subject's wrist with a rubber band.

After a period of dark adaptation (at least 5 minutes) rectangular current pulses were applied to the electrodes; these pulses were delivered by a non-line, transistorized pulse generator.

In all tests a 1:1 ratio was selected for pulse and pause intervals of the current pulses (keying ratio). Use of an oscillograph made it possible to control the excitation parameters, frequency and current pulse amplitude, all of which were to be varied by the tester.

When the measurements began, a medium pulse frequency (20 Hz) was employed and the pulse voltage gradually increased with a potentiometer built into the generator until it reached the point where a subjective flicker was evoked in the test subject. With repeated turning off and on of the current the test subject could get accustomed to observe the appearance and disappearance of the flicker. /5

The actual measurement procedure was as follows. In the frequency area

from zero to 50 HZ test frequencies were applied at intervals of 2.5 Hz. At each of these frequencies the voltage was increased gradually to the point where the test subject signaled appearance of the flicker. In order to keep excitation exposure as short as possible (this to prevent fatigue phenomena), the tester turned the current off again. He then recorded on the sheet the oscillograph reading for the threshold value of the excitation voltage. For each test frequency the excitation threshold was measured a number of times (3 to 5 times). Later the average value as well as the statistical scattering was calculated from the voltages measured for each test frequency and mapped on a frequency-voltage diagram.

2. Results

2.1. Frequency Dependence of Flicker Threshold for Test Subjects of One Control Group

In the case of four test persons of one control group the flicker threshold was measured at time intervals of several months. The resulting threshold curves are given in Figures 2 through 5. The later measurements are de-

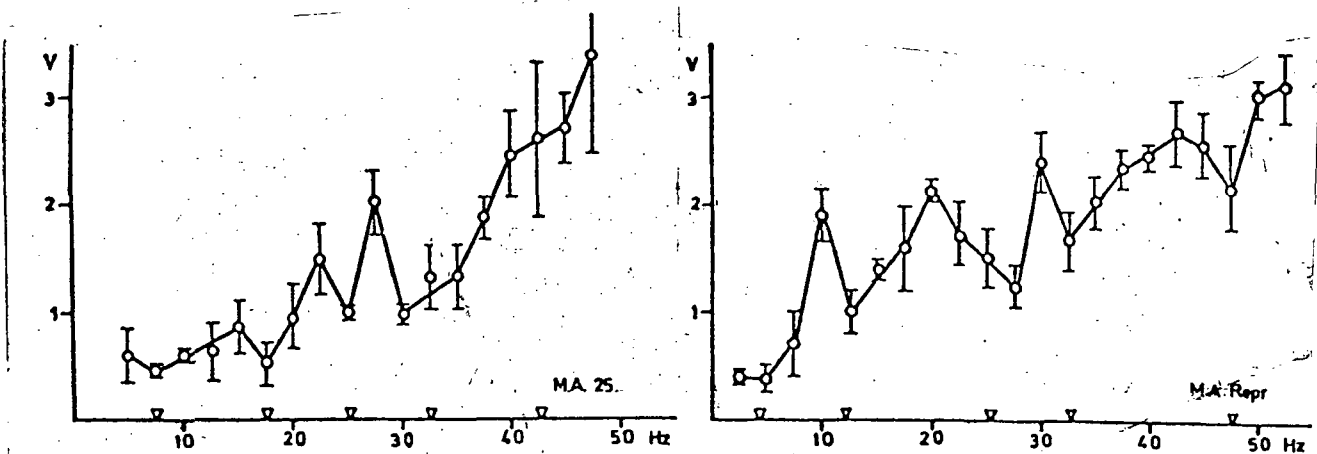


Fig. 2. Frequency-voltage diagrams for subject M.A.

signed by Repr. (reproduction tests).

All threshold curves for the control group show distinct minima (marked with an inverted triangle) at frequencies which at first sight appear to have a harmonious numerical interrelation. This would necessarily mean, that the minimum frequencies can be represented by whole multiples of a basic frequency. Mathematically expressed such a ratio would be

$$f_n = f_0 \cdot n$$

($n = \text{integers}$, $f_0 = \text{basic frequency}$, $f_n = n \text{ th minimum frequency}$).

Figures 6 a-d show that this interrelation may be regarded as a good approximation.

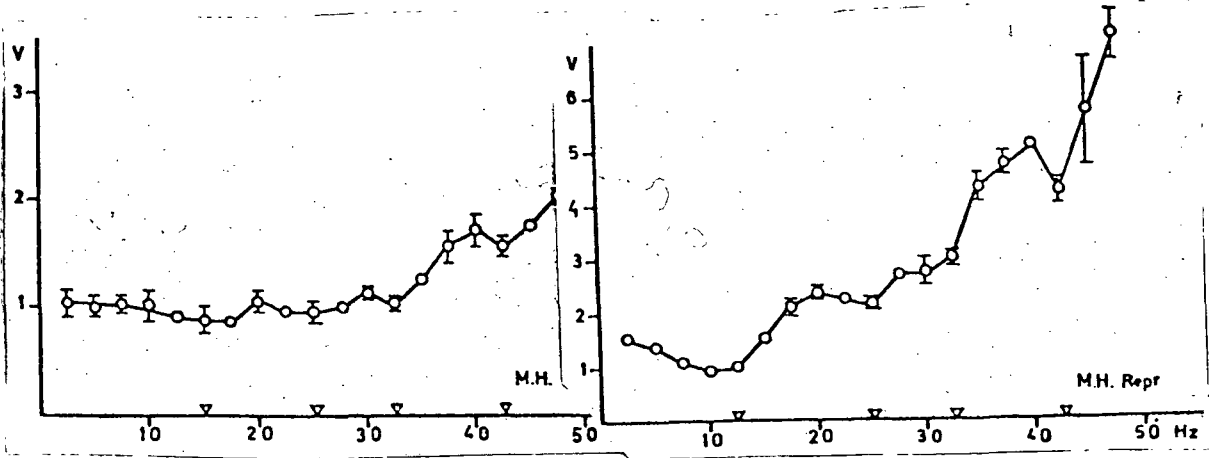


Fig. 3. Frequency-voltage diagrams for subject M.H.

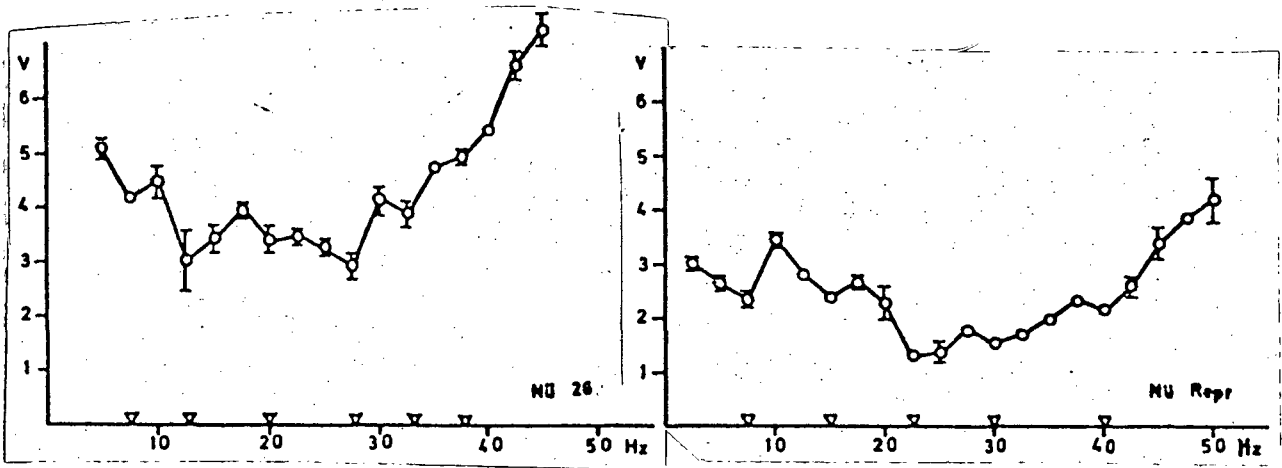


Fig. 4. Frequency-voltage diagrams for subject Nü.

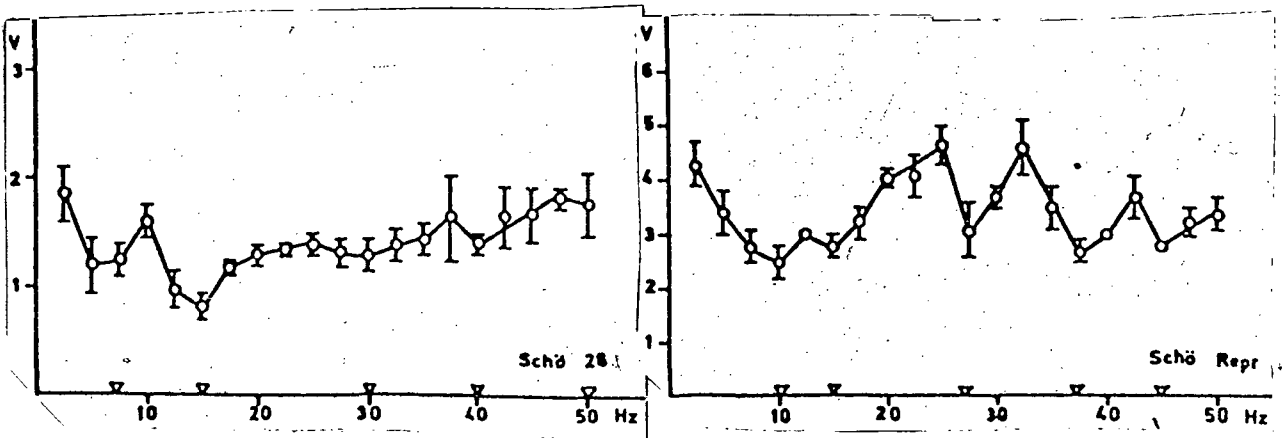
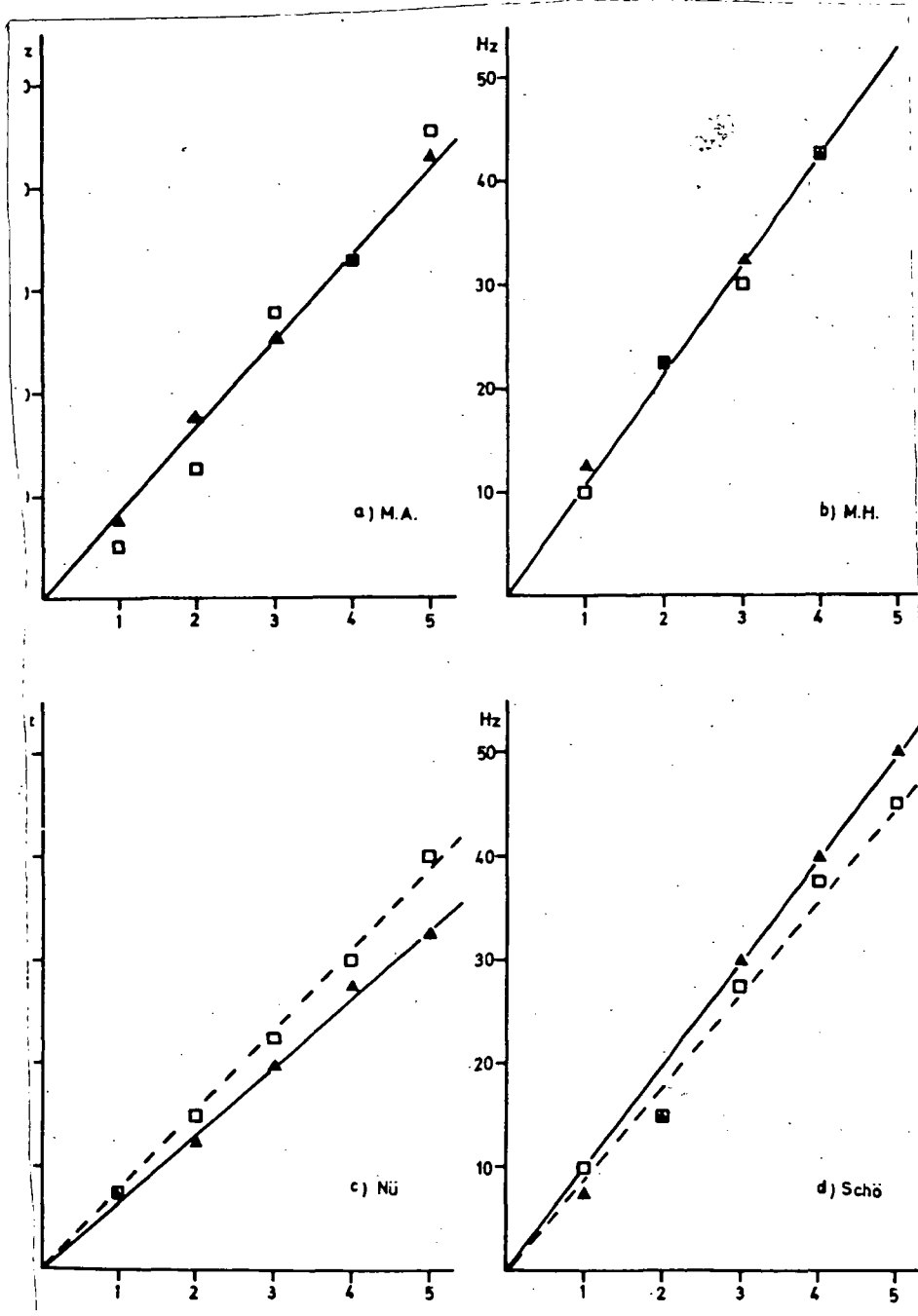


Fig. 5. Frequency-voltage diagrams for subject Schö.



Figures 6 a-d. Proof of harmonious interrelationship between minimum frequencies of control group

The minimum frequencies taken from the threshold curves are plotted against the first integers. The measurement points obtained (solid triangle for the first measurement and empty square for the reproducing measurement) form nearly straight lines that pass through the zero point of the diagram. The slope of such a straight line gives the basic frequency f_0 . One notices, that there is very little change in the basic frequency for a given subject over several

months. Thus, practically speaking, they may be considered as individual constants.

Another mutuality seems to reside in the tendential course of threshold curves for higher frequencies: excitation voltage rises constantly with increasing excitation frequency, so that each of the threshold minima is a bit higher than its predecessor. This may be stated particularly for the threshold curves given in Figures 2 and 3. The difference between these curves and those of Figures 4 and 5 lies only in the fact, that the latter show another slight rise for small frequencies, as shown by the records of subject Nü, or go up very slowly in response to higher frequencies, as is seen for example in the curves of subject Schö.

It merely remains to point out, that in the case of subjects M.A. and Nü it was possible for the subject himself to apply the threshold voltage, while the tester limited himself to applying a given pulse frequency by means of the oscillograph and to put down in the test record the threshold voltage values indicated by the oscillograph.

In summary: when electric excitation pulses are applied to the eye, their effectiveness, indicated to test subjects by the occurrence of flicker phenomena, is not merely a function of the strength of the excitation pulses. The frequency at which the pulses succeed one another is also important. The translation of electric pulses into subjective observable phenomena of an incipient flicker seems to occur preferentially at those excitation frequencies which have proved to be whole multiples of a basic frequency. We designate this as harmonious frequency filter behavior. /10

Investigations done on patients with injuries to the visual nervous system should identify the site in such a frequency filter arrangement which determines this frequency filter behavior.

2.2. Frequency Dependence of Flicker Threshold for Test Subjects with Pathological Changes of the Retina

We start out from the assumption, that the retina is responsible for the translation behavior found. In that case several layers of nerve cells (neurons) become candidates for the role of filter mechanism site.

Macroscopically the retina comprises three superimposed cell layers (epithelia): receptor epithelial cells, bipolar cells and ganglion cells (Fig. 7). The cells of one layer are in neural contact with the next epithelial layer via the so-called axons. Light falling on the retina excites the receptor cells exclusively, whereupon the latter send out electric impulses to the bipolar cells. These then transmit such excitation impulses to the ganglion cells, which finally communicate neural impulse volleys to the brain via their axons (fibers of the optic nerve).

In the case of our experiments we used as a point of departure the idea, that the electric excitation current is capable of stimulating all layers of the retina to the same degree. Thus investigation of patients presenting exclusive impairment of a single retinal layer should make it possible to select /11

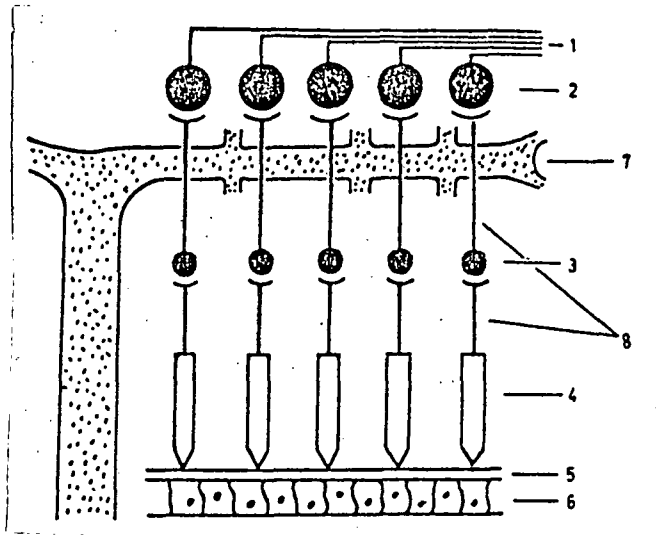


Fig. 7. Schematic presentation of the retina and its supply systems. 1 - optic nerve fibers, 2 - ganglion epithelium, 3 - bipolar epithelium, 4 - receptor epithelium, 5 - choroid, 6 - pigment epithelium, 7 - blood vessel system, 8 - axons

clusion of the blood vessels for example selectively disconnects the layers of the bipolar and ganglion cells.

The patients being studied were therefore divided into these two groups: patients with impairment of the receptor epithelium and patients with injuries of the central nervous retina layers or of the optic nerve.

Figures 8 and 13 are a schematic representation of the clinical pictures for patients belonging to these main groups of retinal diseases.

It may be of fundamental importance for the interpretation of measurement results, what dimensions and what configuration are exhibited by the injured portions of the layer. Therefore, in addition to the division into injuries to receptor epithelium and injuries to the central nerve layers, we used a further differentiation of the above two groups into these subgroups:

- 1) total or nearly total impairment of a layer
- 2) partial, central impairment of a layer (central scotoma)
- 3) unilateral impairment of a layer

We added drawings of the fundus or perimeter sheets to the flicker threshold curves. In these representations hatched areas show damaged regions.

As in the case of measurements done on test subjects of the control group, we will be able to evaluate threshold curves from patients with retinal injuries on the basis of the two following criteria:

the particular epithelium which in a given case would be considered to be the seat of the frequency filter mechanism.

The ophthalmological differentiation of impaired retinal layers is done, among other circumstances, according to the following point of view: the receptor epithelium on the one hand and the layers of bipolar and ganglion cells on the other (central nervous retinal portions) are nourished in different ways. Whereas the receptor cells share metabolism with pigment cells and the adjacent choroid, the central neural retina layers are taken care of by the blood vessels (see Fig. 7). If, for example, metabolism between pigment epithelium and receptor epithelium is interrupted (due to detachment of the retina from the pigment epithelium), only the receptors are functionally impaired. On the other hand, an oc-

/12

1. Occurrence of threshold minima at excitation frequencies which in a given case once more satisfy a harmonious relationship.

2. Tendential course of the threshold curve, which can be represented by setting a polygonal course through the minimum points of the voltage-frequency diagram (broken line). As the norm we take a chainlike sagging polygonal course having only a single minimum in the vicinity of 20 Hz (see course of curves for control group).

/13

For each of the following test groups the results are synthesized on the basis of these two criteria.

2.2.1. Injuries to the Receptor Epithelium

/14

Figure 8 is a schematic representation of the clinical pictures of those retinal disease, which were presented by the test subjects belonging to this group.

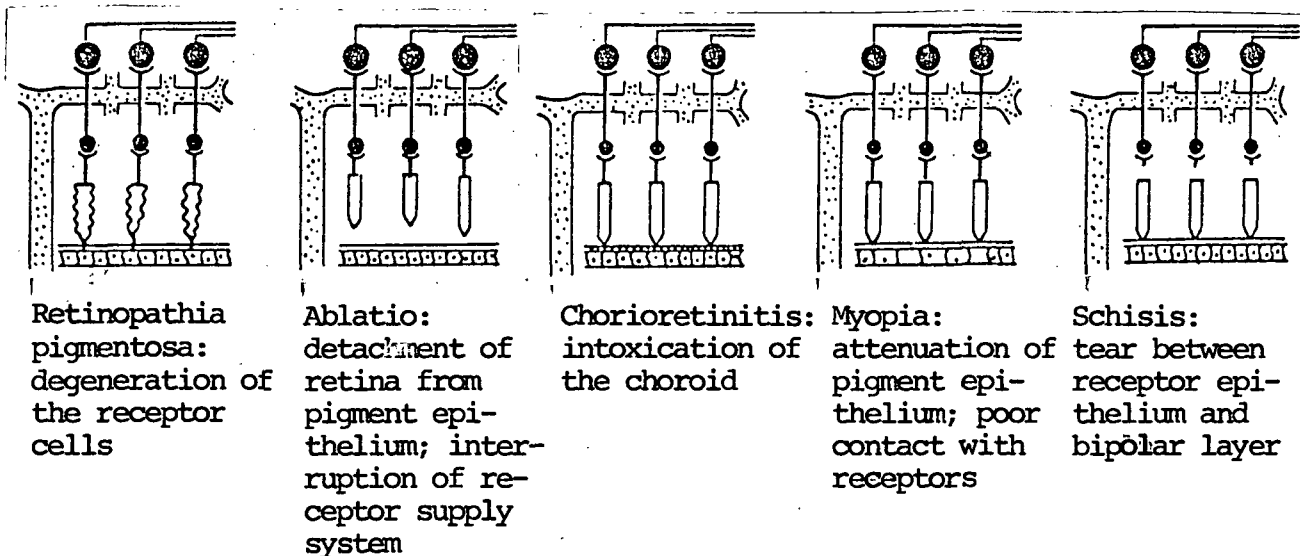


Fig. 8. Schematic representation of pathological impairment of retinal receptor epithelium

a) Total Damage to Receptor Epithelium

/15

Retinopathia pigmentosa

Figures 9a and 9b give the flicker threshold curves for the left (a) and right (b) eye of a female patient (H.H., 25) with bilateral retinopathia pigmentosa. As we see from the hatched portions of the fundus diagrams, the receptor epithelium has degenerated except for small central areas. Nevertheless the flicker threshold curves indicate minima.

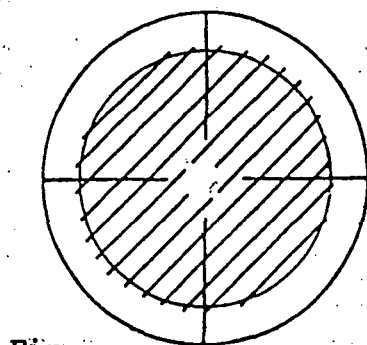


Fig. 9a

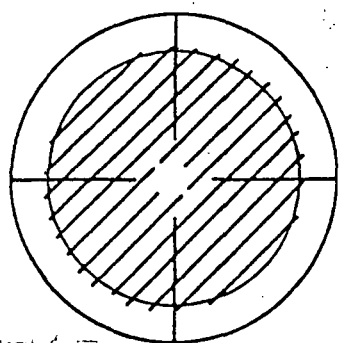
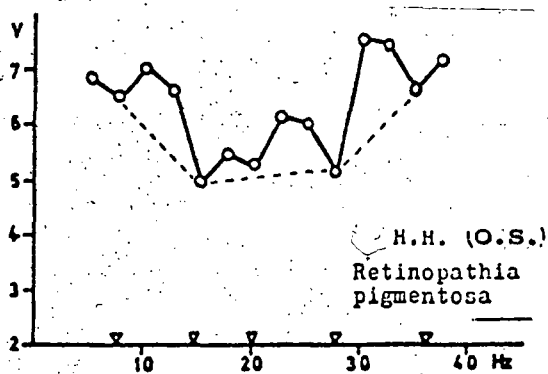


Fig. 9b

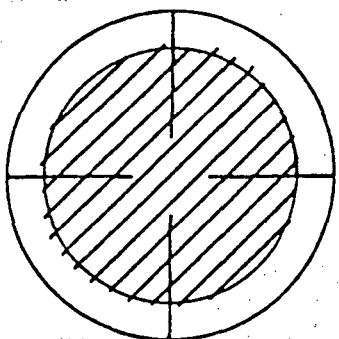
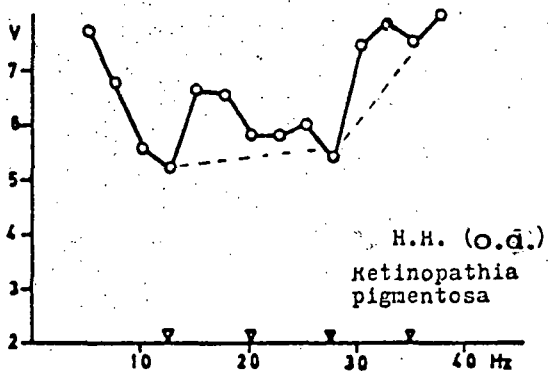


Fig. 9c

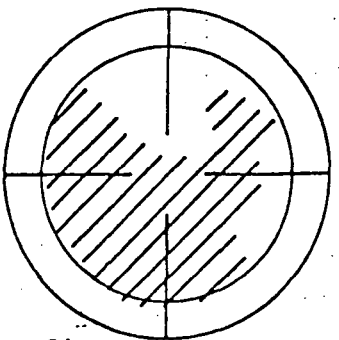
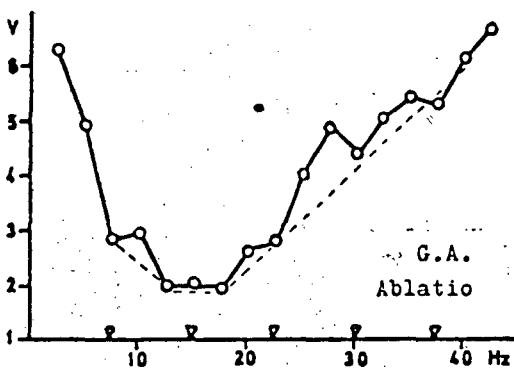
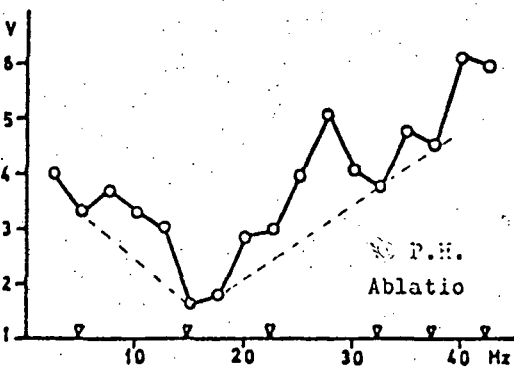


Fig. 9d



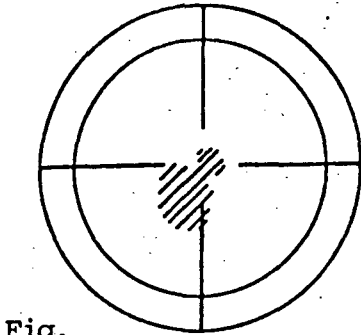


Fig. 10a

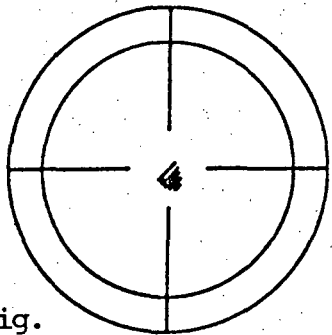
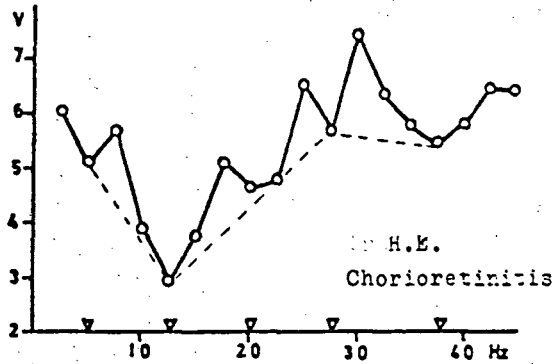


Fig. 10b

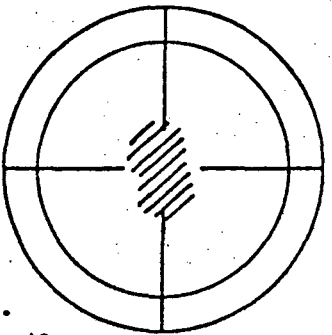
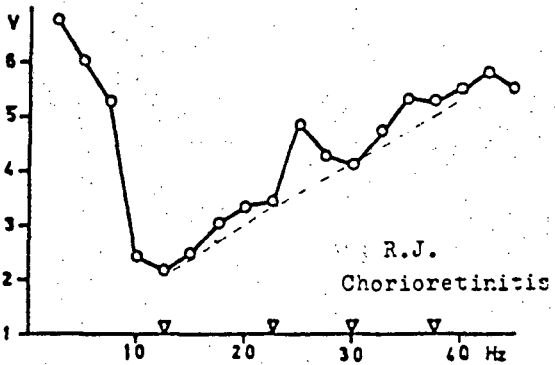


Fig. 10c

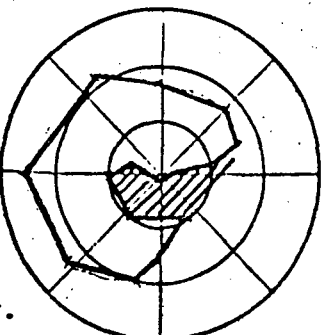
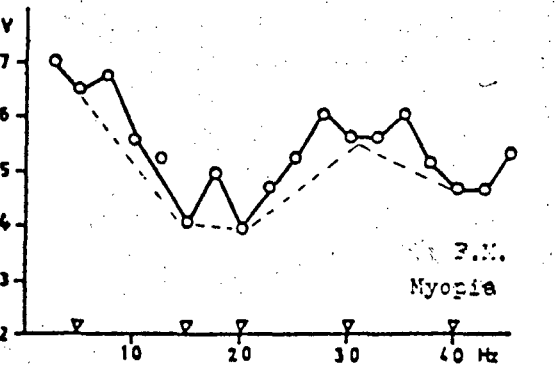
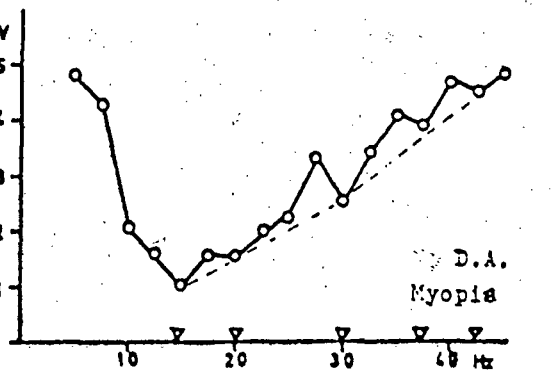


Fig. 10d



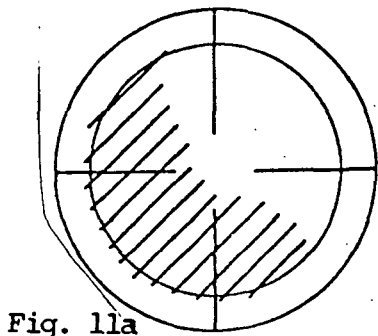


Fig. 11a

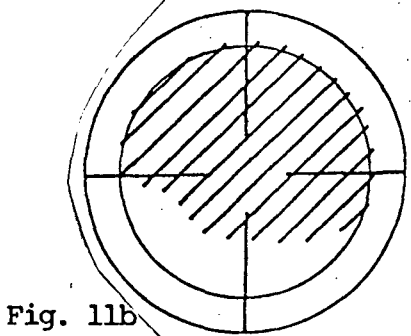
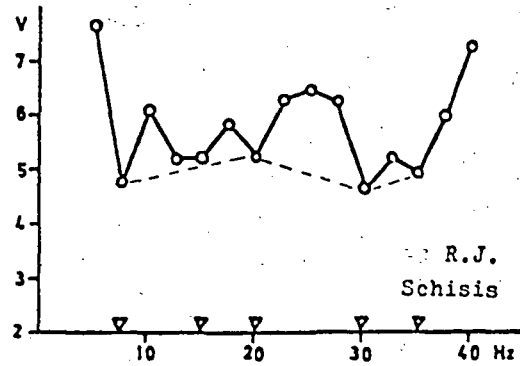


Fig. 11b

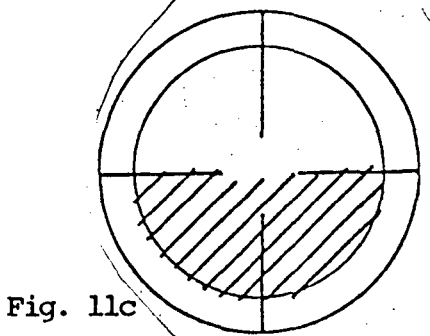
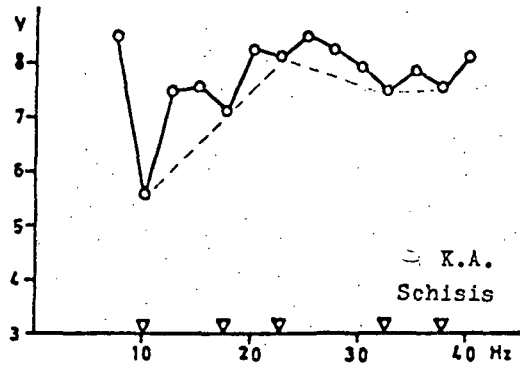


Fig. 11c

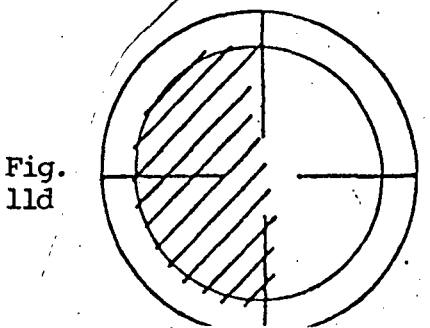
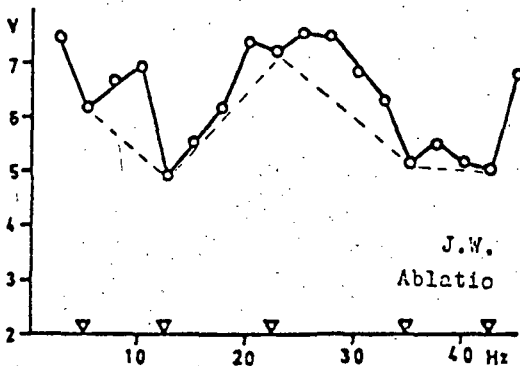
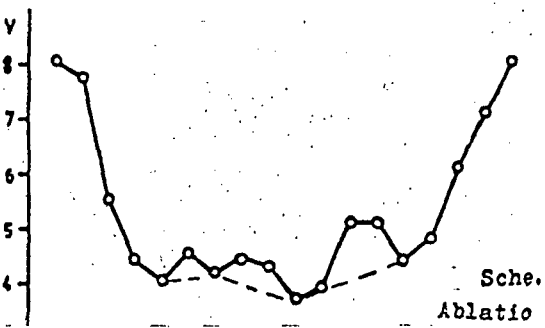


Fig. 11d



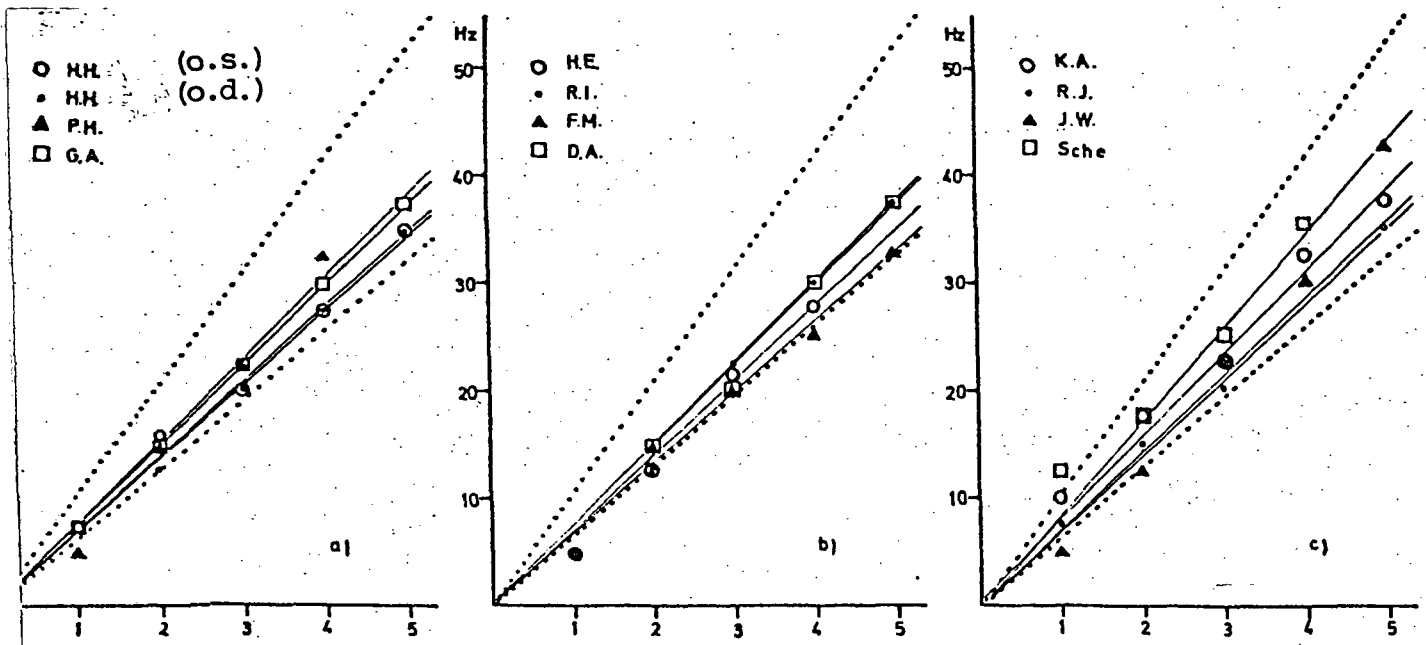
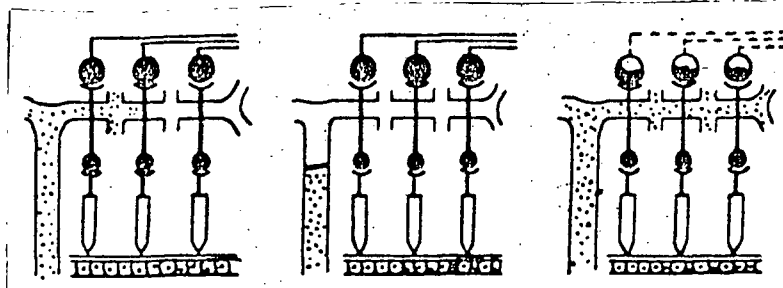


Fig. 12a-c. Proof of harmonious relationship between minimum frequencies for impaired receptor epithelium: a - totally impaired receptor epithelium, b - damaged central areas of receptor epithelium, c - unilateral damage to receptor epithelium



Retinopathia diabetica: poor circulation in central neural retina layers due to arteriovenous shortcircuiting

Vascular occlusion: loss of circulation in the central neural layers

Neuritis: intoxication of the optic fibers and ganglion cells

Fig. 13. Schematic representation of pathological injuries to central neural retina layers

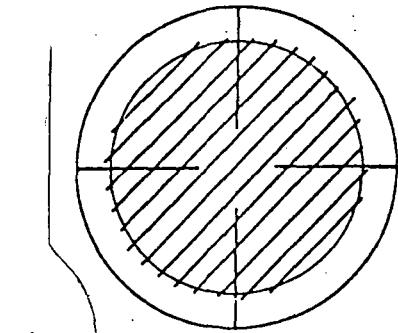


Fig. 14a

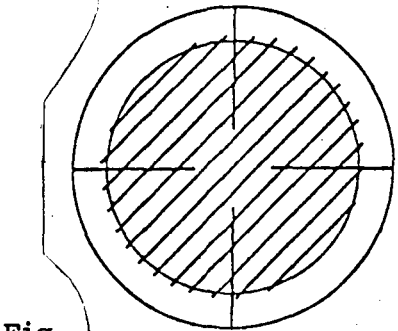
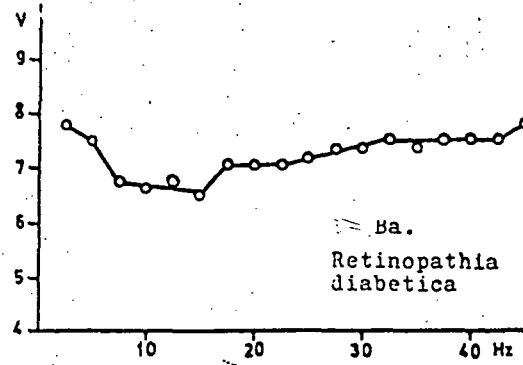


Fig. 14b

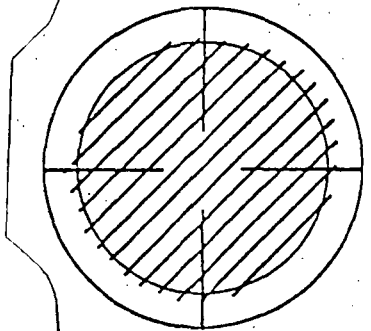
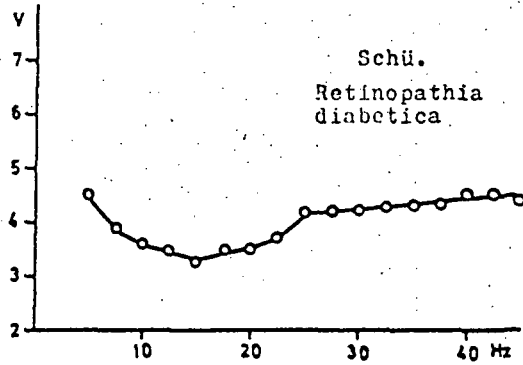


Fig. 14c

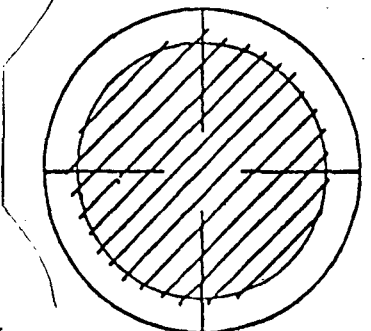
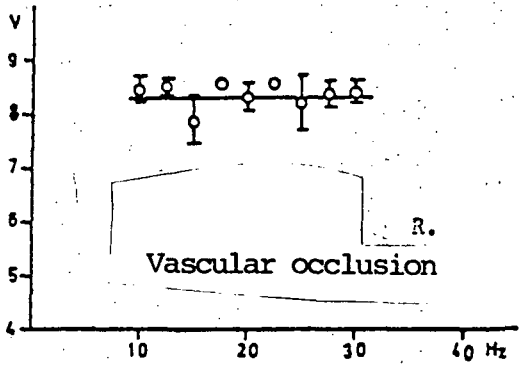
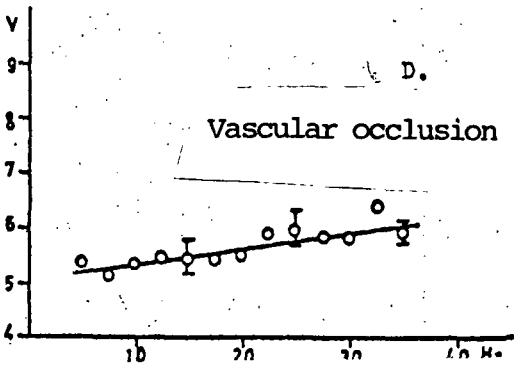


Fig. 14d



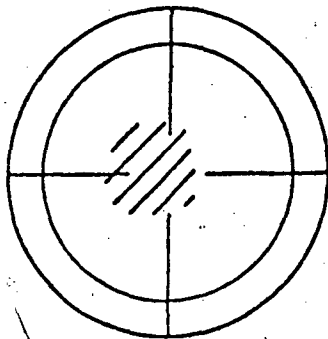


Fig. 15a

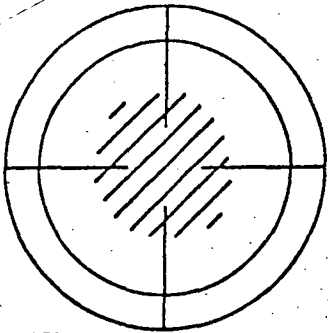
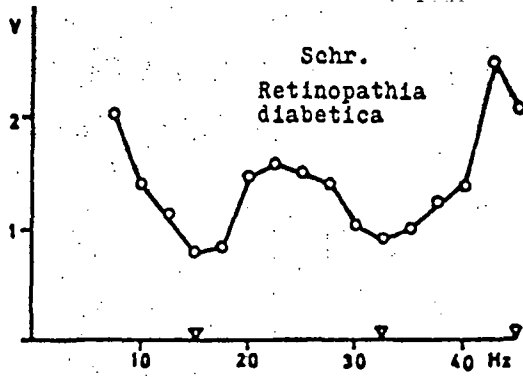


Fig. 15b

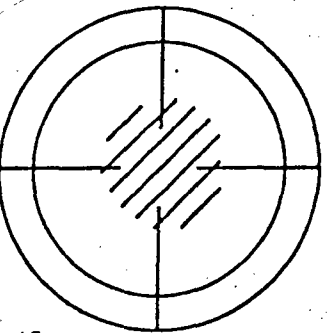
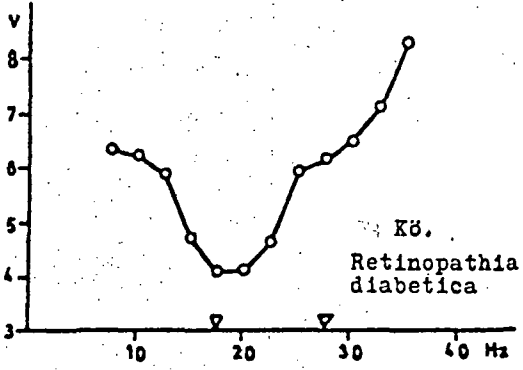


Fig. 15c

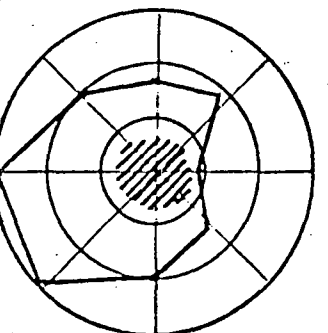
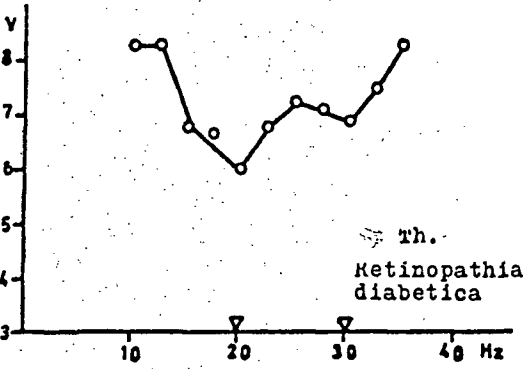
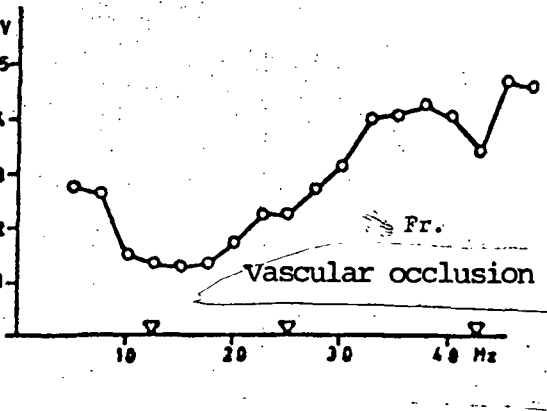


Fig. 15d



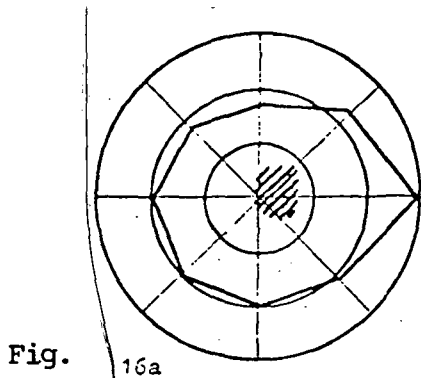


Fig. 16a

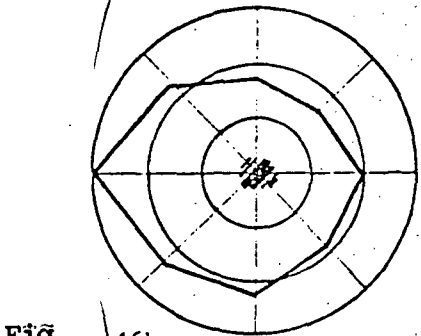
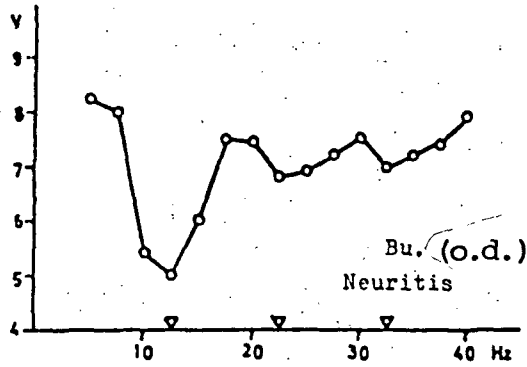


Fig. 16b

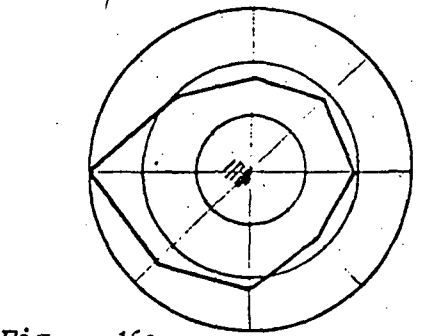
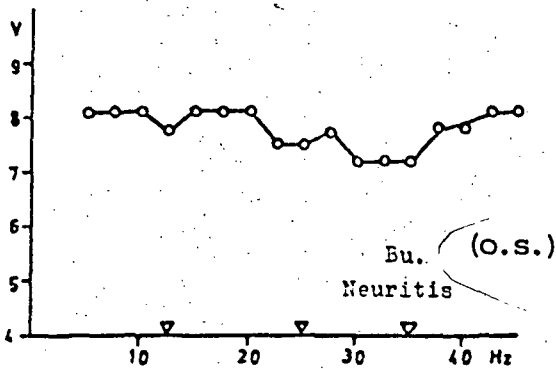


Fig. 16c

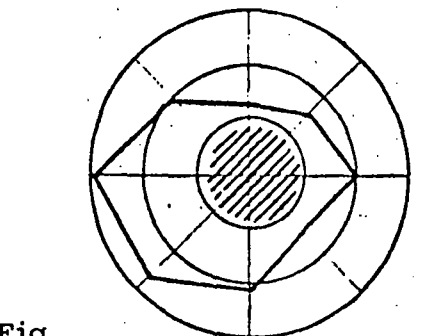
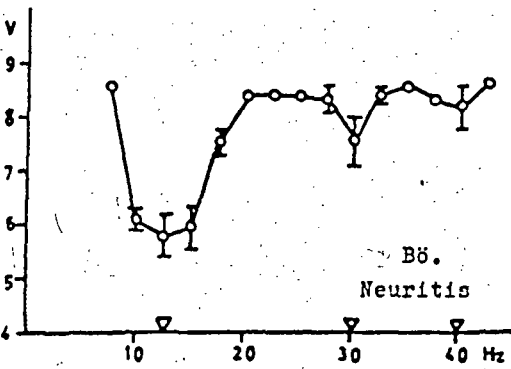
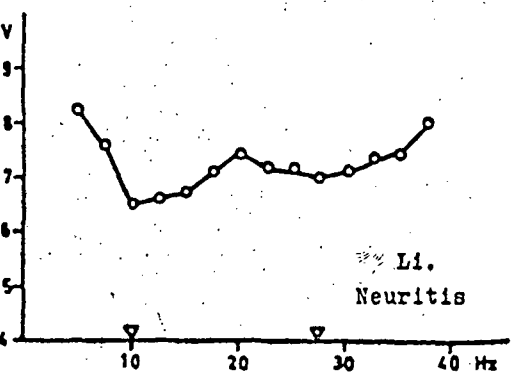


Fig. 16d



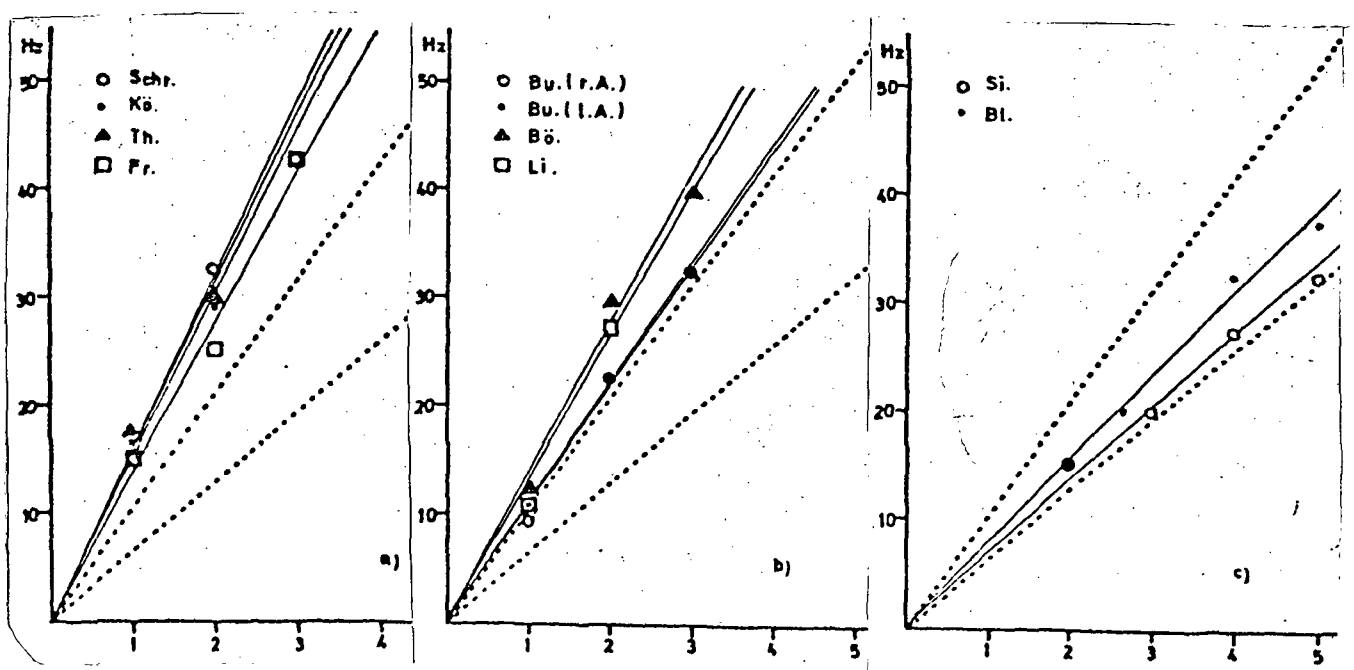
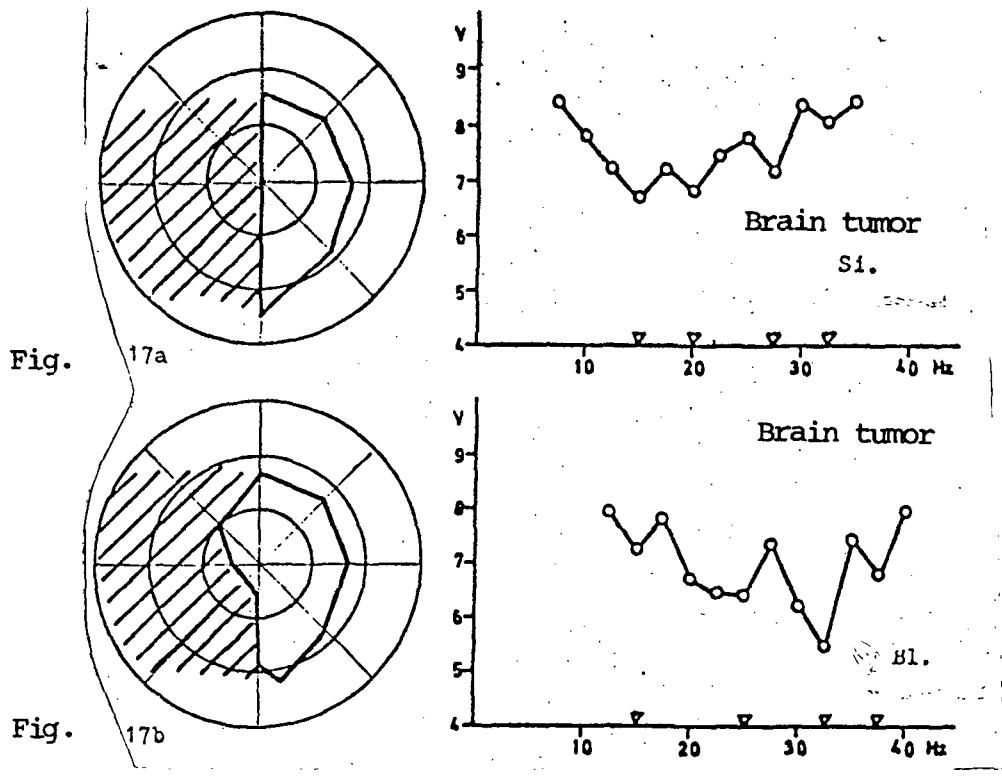


Fig. 18. Proof of harmonious relationship between minimum frequencies for injuries of the central neural retina layers and of higher centers: a - impaired central areas of the bipolar and ganglion epithelium, b - neuritic injuries, c - cerebral processes (brain tumor);

In Fig. 12a the measured minimum frequencies are plotted against the first integers (empty circle for left eye, dot for right eye of the test subject H.H.). The resulting points lie close to a straight line running between the corresponding straight lines of the control group subjects, for whom the greatest and smallest slope was indicated. The last named straight lines thus define the "normal area". Its boundaries are indicated by dotted lines in Fig. 12a. Thus Fig. 12 shows, that in spite of extensive degeneration of the receptor epithelium no deviation occurred in respect to the rule of harmony for minimum frequencies set up in the first instance for unimpaired retinas.

/15

The tendential course of the two threshold curves is likewise normal.

Ablatio

Figures 9c and 9d present flicker threshold curves of two patients (G.A., 50 and P.H., 45) with extensive retinal detachment. The curves of these patients also show minima at frequencies for which in Fig. 12a the test for a normal harmonious relationship could be applied. The measurement points for these test subjects (empty square for G.A. and solid triangle for P.H.) also lie along straight lines within the normal area.

The tendential course is also normal here.

Summarizing:

/17

1. The minimum frequency harmony rule remains intact even in cases of extensive injury to the receptor epithelium.

2. In the cases presented the normal tendential course of the threshold curves (broken lines) is also maintained.

From these findings we conclude, that the layer of the retinal receptors cannot be held responsible for frequency filter behavior.

b) Damage to the Central Regions of the Receptor Epithelium

/18

Chorioretinitis

Figures 10a and 10b show threshold curves for two patients (H.E., 27 and R.J., 26) with centrally located foci of chorioretinitis. In both cases there is also selective damage in the foveal region as well as damage to the cone apparatus.

Once more we find minima in the threshold curves. In the case of the test subject R.J. they seem less pronounced or run together like a plateau (at 22,5 Hz).

The minimum frequencies satisfy the rule of harmony. Their corresponding points of measurement in Fig. 12b (empty circle for H.E. and dot for R.J.) lie along straight lines within the normal range.

While the tendential polygon for test subject H.E. does not continue to

rise as the frequency increases but rather drops again between 30 and 40 Hz, a normally tendential curve can be established for R.J., whose retina shows much less disturbance.

Myopia

In two other patients central areas of the receptor epithelium were damaged due to myopic attenuation of the corresponding sites in the pigment epithelium.

Their threshold curves as presented in Figures 10c and 10d likewise show minima. The frequency values associated with the minima are in accord with the rule of harmony, as appears from Fig. 12b.

However, when observing the tendential polygons we find, that damage to a rather large central area disturbs the tendential course. Thus the tendential polygon for test subject F.M. also goes down between 30 and 40 Hz instead of rising constantly.

Summarizing:

1. Impairment of the foveal area of the receptor epithelium (selective disconnection of the cone apparatus) leaves the rule of minimum frequency harmony intact.

2. If the damaged central areas of the receptor epithelium are small, the corresponding threshold curves also show normal tendential polygons with a single minimum at 15 Hz. If there is damage to more extensive central areas of the receptor epithelium, the tendential curve drops again between 30 and 40 Hz.

The results establish on the one hand that some neural structure other than the receptor epithelium must be responsible for the formation of the threshold minima. On the other hand they do indicate some influence of the receptors on such a structure, inasmuch as more significant losses of the central receptor epithelium are reflected in an anomalous tendential course of the threshold curve.

c) Functional Disconnection of Half the Receptor Epithelium

Schisis

Figures 11a and 11b contain threshold curves of two patients (R.J., 30 and K.A. 68) with approximately unilateral schisis areas. In viewing the hatched fields in the fundus diagrams one should picture the central nerve layers as lifted off the receptor epithelium. Consequently the bipolar and ganglion cells in these areas are no longer innervated by the receptors.

The frequencies corresponding to the threshold minima were plotted in Fig. 12c against the first integers. The resulting points (empty circle for K.A. and dot for R.J.) lie along straight lines within the normal range. For both patients however the tendential polygon deviates from a normal course.

/20

/21

Ablatio

Figure 11c-d shows threshold curves for two patients (J.W., 45 and Sche., 55) with unilateral ablatio. The points answering to minimum frequencies in Fig. 12c (J.W. ▲, Sche. □) define straight lines with normal slope. However, the tendential course is not normal.

In summary: 1. Unilateral losses of receptor epithelium change nothing in respect to the rule of harmony for minimum frequencies; 2. In all cases of unilateral loss of receptor epithelium the tendential polygon runs an abnormal course.

Here again we find support for our assumption, that partial losses of the receptor layer can influence only the tendential course of the flicker threshold curve. Frequency filter behavior must be ascribed to some other neural system of the visual organ.

2.2.2. Damage to the Central Neural Retina Layers and Optic Nerve (Bipolar and Ganglion Epithelium)

/24

Fig. 13 shows the clinical pictures of the retina diseases presented by the test subjects of the group under discussion in a schematic way.

a) Total Impairment of Central Neural Retina Layers (Bipolar and Ganglion Epithelium)

Retinopathia diabetica

Figures 14a and 14b show threshold curves for two patients (Ba., 45 and Schü., 55) with advanced retinopathia diabetica. Patients with this disease develop arteriovenous short circuits in the retinal blood vessel system, so that the neural layers show deficient circulation. This causes functional disturbance of the bipolar and ganglion layer.

The pictures of the flicker threshold curves have now radically changed: no significantly distinct threshold minima are to be observed. The course of the tendential curve is well nigh horizontal.

Total Vascular Occlusion

Figures 14c and 14d represent threshold curves of patients (R., 49 and D., 60) with closed retinal central arteries. The result was interruption of circulation in the central neural retina layers. Both patients were totally blind in the affected eye.

The threshold curves showed no appearance of minima. The tendential curve ran an almost horizontal course.

Summarizing:

1. Total damage to the central neural portions of the retina cause the disappearance of all threshold minima.

2. The course of the threshold curve is almost horizontal.

The visual organ therefore loses its quality of frequency filter, the moment that damage to the central neural retina layers is total. From the horizontal course of the threshold curve we conclude, that the excitation threshold is no longer a function of the excitation frequency.

We can thus narrow the search for the seat of the frequency filter down to one of the two central neural layers, the bipolar epithelium or the ganglion epithelium.

b) Impairment of Central Regions of the Bipolar and Ganglion Layer

/27

Retinopathia diabetica

In the case of three test subjects damage due to retinopathia diabetica remained confined to central areas of the central neural retina layers. The threshold curves of these subjects indicate, as we see from Figures 15a, b and c, the presence of distinct minima once more, though they seem to be spaced farther apart perhaps than was the case with the control group. If, as has been done in Fig. 18a, we plot the minimum frequencies against integers, we once more get straight lines connecting the corresponding diagram points (empty circle for Schr., 39 and a dot for Kö., 45 and a solid triangle for Th., 65) and the starting point of the coordinate system. However all the slopes of these straight lines lie higher than the norm. Thus the basic frequency f_0 has increased. Herewith the entire spectrum expands, but the curve tendencies remain normal.

Vascular Occlusion

In the case of the subject Fr. an occlusion of the central artery had caused loss of the middle visual field. Here likewise the minimum frequencies obtained were plotted in Fig. 18a against the first integers. The corresponding points (empty square) also define a straight line with an abnormally steep slope.

The tendential course is nevertheless normal.

Summarizing:

Injuries to central areas of the bipolar and ganglion epithelium condition a rise in the basic frequency f_0 and accompanying broadening of the entire spectrum of minimum frequencies.

c) Loss of Central Visual Field due to Neuritic Impairment of the Optic Fibers

/29

The four threshold curves in Figures 16a-3 were measured on patients with central scotomas for which neuritic damage to the optic nerve was held responsible. Instead of fundus diagrams perimeter sheets are used here. The outer limits of the visual fields are marked and into them are inserted (hatching) the scotoma areas.

All threshold curves contain distinct minima in which we once more observe

expansions of the corresponding spectra: plotted against the first integers the minimum frequencies in Fig. 18b define straight lines, whose slope lies outside the norm in every case without exception.

The diagram points of the three test subjects are identified as follows: empty circle for the right eye and a dot for the left eye of Bu, 53; solid triangle for Bø, 50 and empty square for Li, 50.

Curve tendencies are always normal.

Summarizing:

Neuritic injuries to optic nerve fibers with origin in a central area of the ganglion epithelium cause a repetition of that effect of an expansion of the entire spectrum, which we had already found in cases of similar damage to the two central neural layers (bipolar epithelium and ganglion epithelium).

Since the optic nerve fibers represented the axons of the ganglion cells, we may assume, that neuritic intoxication of the fibers spreads to the ganglion cells. This means then, that injury to the ganglion epithelium alone (without injury to the bipolar cells) effects that modification of frequency filter behavior. Spectrum expansion seems to be all the greater as the radius of the damaged central area is larger.

2.3. Loss of Visual Field due to Cerebral Processes

/31

Figures 17a and 17b contain the threshold curves of two patients where unilateral visual field losses were considered the result of pathological changes in the extraocular higher layers of the visual nervous system. In both patients the retinas were intact.

The minimum frequencies of the threshold curves define diagram points in Fig. 19 (empty circle for Si. and dot for Bl.) that lie along straight lines with normal slope.

Summarizing:

Injuries to extraocular centers of the visual nervous system do not affect the frequency filter behavior of the visual organ. Therefore this behavior must be ascribed to the retina and in particular to the ganglion epithelium.

3. Discussion of Experimental Investigations

/34

The increased excitability of the visual nervous system in respect to electric pulse series of harmonious frequencies, as was expressed first of all in the threshold curves of the control group, is reminiscent of a resonance mechanism. Thus the following concept presents itself as a hypothesis for the interpretation of flicker threshold curves: the visual nervous system contains a nerve structure (for example an assemblage of neurons) capable in their activity of producing a certain harmonious "natural oscillation."

The occurrence of such "natural oscillations" might be induced by the functional architecture of this neuron assemblage, since it allows the exchange of pulse volleys between neurons to take place only in a specific rhythm. If alternating excitation currents engage a neuron assemblage of this sort, it is possible for them to stimulate the cells with special intensity whenever the excitation pulse frequency attains a unison with the "natural rhythm". If the pulse series brought the neuron assemblage to an excitation level to which the production of a subjective flicker might perhaps be attached, pulses having one of the "natural frequencies" would not have to be as intense for this purpose as those of other frequency series. This involves a qualitative interpretation of the frequency filter behavior.

The hypothesis of a neural resonance mechanism implies the question as to where it is located in the human visual organ. We might expect an answer from measurements on patients with impairment of specific areas of the visual nervous system, because every selective injury of that resonance apparatus ought to be recognizable by the disappearance of the threshold minimum or by modifications of the "natural" frequencies.

We could never observe changes in the spectrum of "natural" frequencies for patients with exclusive impairment of the receptor epithelium. This eliminated the receptor epithelium as the seat of the frequency filter mechanism. However, on the basis of measurements done on patients with central and unilateral loss of the receptor layer, it must be freely admitted, that the photoreceptors are capable of influencing the frequency filter. If the damaged areas had been more extensive, it would have been regularly possible to establish an abnormal tendential course taken by the flicker threshold curve. /35

We first observed radical changes in the curve of the flicker threshold for patients with impairment of the central neural portions of the retina. In cases of extensive degeneration areas there was no longer a sign of threshold minima. Thus in cases of impairment of the central neural portions of the retina the frequency filter property was lost.

However threshold minima reappeared, as soon as the damage was only to central areas of the bipolar and ganglion layer. In such cases the minimum frequencies even satisfied a harmonious relationship, but the basic frequency f_0 was always higher than the largest value obtained from a test subject of the control group. The broadening thereby of the total spectrum will be of interest in the theoretical considerations.

The reason for loss of central neural layers was in all cases an interruption or diminution of blood circulation. Since this affected both layers of the central neural apparatus of the retina, namely bipolar cells and ganglion cells, to the same degree, we were not yet able to decide in which of them we ought to locate the seat of the frequency filter.

However, with the help of patients in whom a visual impediment was to be traced to neuritis, we succeeded in making the definitive selection of that epithelium, which alone may be regarded as the seat of the resonance mechanism. This disease consists in an intoxication of the optic nerve fibers. Since the latter represent the axons of the ganglia, it is plausible to assume that such intoxication spreads to the ganglion cells.

The flicker threshold curves for patients with central visual field losses imputable to a neuritis are very similar to the threshold curves we had obtained in cases of central impairment of the bipolar and ganglion cell layers. Here too we noticed an expansion of the total spectrum. From this we may conclude, that the ganglion epithelium of the retina is alone the host of the frequency filter mechanism.

/36

The argument, that the frequency filter might also be located outside the retina at a higher level of the visual nervous system, is invalidated by our finding, that a normal frequency filter behavior may be demonstrated for patients whose visual field losses were due to cerebral processes.

Now that the retinal ganglion epithelium has been shown to be the seat of the frequency filter, we will attempt in the theoretical portion of this work to interpret the findings of the experimental investigations by means of a system model of the ganglion layer.

IV. Theoretical Interpretation of the Retinal Frequency Filter Property in respect to Alternating Electric Currents Using a System Model of the Ganglion Layer

/37

1. Definition of the Problem

The frequency dependence of the excitation threshold for electrically stimulated subjective flickering expressed frequency filter behavior of the retina. This behavior was characterized by excitation threshold minima that occurred at whole multiples of a basic frequency ($f_0 = 8\text{Hz}$). It was possible to demonstrate modifications of these minimum frequencies exclusively in test subjects with pathological changes of the central neural portions of the retina and especially of the ganglion epithelium.

It is therefore natural to ascribe to the retinal ganglion epithelium the transfer property that determines the course of the flicker threshold as a function of the excitation frequency.

For the theoretical interpretation of the experiments, in which the statements of test subjects in respect to the occurrence of subjective flicker phenomena were correlated with parameters of the excitation current (frequency and voltage of the excitation pulses), the following facts are important:

a) The strength of the electric excitation pulses (like the intensity of light stimuli) is signaled by the stimulated neurons of the ganglion epithelium by correspondingly close volleys of short neural impulses, so-called spikes (lasting 1 msec). (Digital reading of stimulus strength) [5,6,7]

b) Dark-light perception correlates with frequency modulations of the spike volleys generated by the ganglion cells of the retina [5].

In line with these findings the framework for a theoretic model will be set up as follows: by means of a mathematical description of neural interactions, which the cells of the ganglion epithelium are capable of producing in their dendrite areas, we may derive a differential equation, which makes

it possible to calculate the distribution of spike frequencies within the ganglion layer spatiotemporally at predetermined stimulation patterns. The correlation between the spike frequency of the ganglion cells and the subjective light-dark sensation will then make possible a qualitative translation of the retinal activity pattern into the statements of the test subjects.

/38

2. Mathematical System Model of the Retinal Ganglion Epithelium

The required theory must take into account the following insights into the histological and functional development of the ganglion layer:

1) The ganglion cells are divided into light-activated and dark-activated neurons (on- and off-neurons) according to their reaction to illumination and darkening. In this arrangement light sensation corresponds to an increased spike frequency of the on-cells, whereas subjective darkness is associated with an increase of off-activity. Moreover the occurrence of on- and off-cells is quite frequent [5,6,7].

2) The dendrite areas of adjacent ganglion cells overlap, so that the individual cells seem to be interwoven in a coherent network through which they can mutually interact in stimulating or inhibiting fashion [11].

3) This ganglion network is interspersed with a further type of neuron, the amacrines, which certainly contribute to neural interchange within the dendrite plexus [11].

Since even recent literature contains no statements about the distribution of stimulating and inhibiting connections between the individual types of neuron, we must achieve a theoretical specification in this regard. These stipulations about the nature of neural interactions thus take on the character of axioms, which are justified by the experimentally established consequences of the system model based upon them.

The proposed model was based upon the following axiomatic assumptions in respect to the interactions of on- and off- ganglions as well as amacrines:

/39

1. Nerve impulses from the receptors (communicated via the bipolar cells turned on between the receptors and ganglion cells) simultaneously excite on-ganglia and inhibit off-ganglia.

2. On- and off-ganglia stimulate their own kind; on the other hand we find no interaction taking place between on- and off-cells.

3. On- and off-ganglia stimulate amacrines but both are inhibited by the latter (brake effect of amacrines).

For a stepwise derivation of a mathematical formulation we take our direction from Fig. 20, in which the connections of the various cells are represented.

In the first step of our derivation we concentrate exclusively on the stimulating interaction between ganglion cells of the same type. In conformity with the retinal ganglion epithelium we imagine a circular disc evenly populated by on- and off- type neurons. At the same time ganglion cells

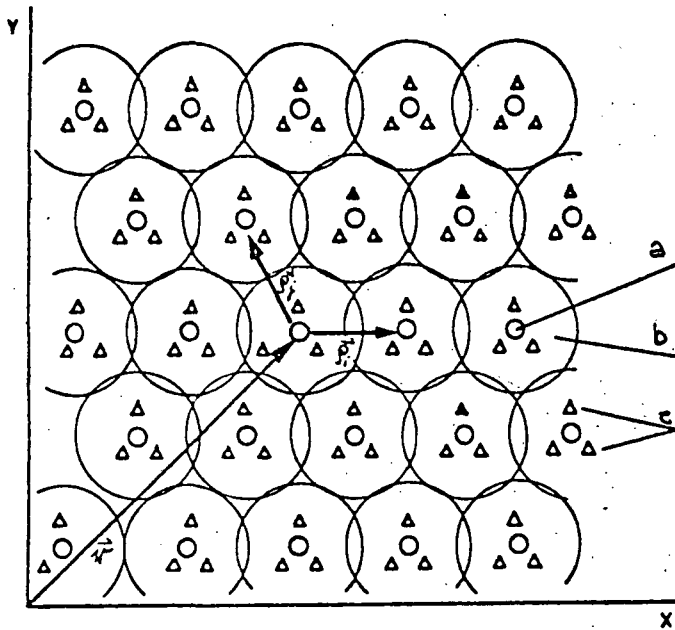


Fig. 20. Schematic representation of the neuron structure of ganglion epithelium
 Key: a - ganglion cells, b- dendrite area, c - amacrines

would be so dense, that the dendrite areas of adjacent cells overlap. With the exception of the cells of the perimeter area of the circular disc every cell in the middle would at the same time have many neuron neighbors. We will call the average number of adjacent cells the "coordination number".

When a ganglion cell generates a nerve impulse (spike), it is communicated as a neural excitation via the dendrite plexus to adjacent ganglion cells in all directions and this induces each of these cells to send out a spike of its own. Thus each ganglion acts as a "source of stimulation". Conversely, each cell must be regarded as a "focus of stimulation", since it is the point of convergence for spikes from its ganglion neighbors.

In working with the theory we must keep in mind, that it is possible for a spike to be damped down to a subliminal amplitude due to a current in the dendrites which is affected by decrement, so that the spike is no longer able to activate its target neuron.

We now take a look at a cell in the laminar ganglion assemblage. Let its position within the epithelium be marked by a planar position vector \vec{r} (see Fig. 20). Further vectors $-\vec{p}_i$ attached to its point would mark the positions of the adjacent ganglion cells. The length of such a vector corresponds to the average distance between two ganglion cells. The amplitude would be estimated at several hundred microns [11].

/40

In a small test interval around time point t let the ganglion fire at position $\vec{r} + \vec{p}_i$ a volley of $\sigma(\vec{r} + \vec{p}_i, t)$ impulses. On their way to the cell located at point \vec{r} some of these impulses are lost due to the decrement-affected current in the dendrites. Thus, of the set of impulses originally sent out, only $\epsilon \cdot \sigma(\vec{r} + \vec{p}_i, t)$ impulses are capable of stimulating the cell at point \vec{r} . The factor ϵ in this case represents the percent loss of spikes.

/41

All told $\sum_{i=1}^N \epsilon \cdot \sigma(\vec{r} + \vec{p}_i, t)$ spikes per time unit travel from the surround toward the cell in question. In this case N represents the coordination number. If this pulse rate is so small, that the time interval between two spikes remains larger than the absolute refractory period (dead time lasting about five msec) of the ganglion cell, the cell is able to respond to the buildup of each spike with one of its own. However, if the cell is engaged by two supraliminal

in one temporal interval smaller than the absolute refractory phase, the cell can respond to only one spike, the first, while the second does nothing toward activating the ganglion cell. The frequency of these ineffective spikes is therefore the same as the frequency of such coincidences. The number of coincidences occurring during a given time interval is calculated as follows: we had assumed, that the adjacent cell at position $\vec{r} + \vec{\rho}_i$ at time t sends out $\sigma(\vec{r} + \vec{\rho}_i, t)$ spikes per time unit. On the basis of the decrement-affected current in the dendrites only a fraction $\epsilon \cdot \sigma(\vec{r} + \vec{\rho}_i, t)$ would reach the ganglion at position \vec{r} . We may regard the expression $\epsilon \cdot \sigma(\vec{r} + \vec{\rho}_i, t)$ as indicative of the probability that the ganglion cell at position \vec{r} will be excited by its neighbor at position $\vec{r} + \vec{\rho}_i$. Then the probability for coincidence of two spikes, one of which proceeds from the cell at position $\vec{r} + \vec{\rho}_i$ and the other from the cell at position $\vec{r} + \vec{\rho}_j$, is proportional to the product $\epsilon \cdot \sigma(\vec{r} + \vec{\rho}_i, t) \cdot \epsilon \cdot \sigma(\vec{r} + \vec{\rho}_j, t)$. This product shows the frequency of coincidences occurring in a given time unit between the spikes of two adjacent ganglia. The number of those coincidences, which occur within the absolute refractory period, is calculated as follows

$$(1) \quad \Theta_0 \cdot \epsilon^2 \cdot \sigma(\vec{r} + \vec{\rho}_i, t) \cdot \sigma(\vec{r} + \vec{\rho}_j, t)$$

$\Theta_0 =$ absolute refractory period [8]

The overall coincidence rate is obtained finally by summation over all possible cell pairs in the surround:

/42

$$(2) \quad \frac{1}{2} \Theta_0 \sum_{i,j=1}^{N,N-1} \epsilon^2 \cdot \sigma(\vec{r} + \vec{\rho}_i, t) \cdot \sigma(\vec{r} + \vec{\rho}_j, t)$$

If we wish to find out, how many spikes from the neighborhood can possibly be answered by spikes from the cell in question, we must subtract the coincidence quota from the number of all spikes reaching their mark per time unit. If in addition we consider the average duration τ for traveling time of a spike between adjacent neurons, the interaction of ganglion cells is represented mathematically as follows:

$$(3) \quad \underbrace{\sigma(\vec{r}, t + \tau)}_{\text{spike rate of a ganglion cell at position } \vec{r} \text{ at time } t + \tau} = \underbrace{\sum_{i=1}^N \epsilon \sigma(\vec{r} + \vec{\rho}_i, t)}_{\text{total spike rate from surround}} - \underbrace{\frac{\Theta_0}{2} \sum_{i,j=1}^{N,N-1} \epsilon^2 \sigma(\vec{r} + \vec{\rho}_i, t) \cdot \sigma(\vec{r} + \vec{\rho}_j, t)}_{\text{coincidence rate} \cdot \text{number of ineffective spikes of surround}}$$

Up to now we have pictured the circular disc corresponding to the ganglion layer as occupied exclusively by ganglion cells. In the second step of our derivation of a mathematical formulation we also take the amacrine cells into account. Now we picture the plexus formed by ganglion cells as simultaneously interlarded with amacrine cells. (see Fig. 20). Since these cells are less numerous, they do not set up a coherent network, so that we may neglect mutual interaction by the amacrine cells.

We now supplement our considerations on the interaction of ganglion cells by describing the inhibition caused by the amacrines. We once more consider in Fig. 20 those ganglion cells, whose position is marked by the vector \vec{r} . Like each of the other ganglion cells, this cell has a number of amacrines caught in its dendrite area, whose number will remain constant for each ganglion neuron in the middle ("coordination number" for amacrines). In addition to receiving stimulating spikes from adjacent ganglion cells, the cell in question is also made to feel, per time unit, inhibiting spikes from the amacrines assigned to it.

We must give the rate of these inhibiting spikes for the same point in time t , at which the adjacent ganglion cells fire their stimulating impulses. At the later point in time $t + \tau$ the inhibiting spikes reach the ganglion together with the stimulating spikes at position \vec{r} . The spike frequency of this cell (equation 3), obtained when we consider the stimulating ganglion spikes exclusively, is therefore reduced by the rate of the inhibiting amacrine spikes. /43

Since the amacrines are supposed to be activated by the ganglion cells, their overall spike rate at time t will be proportional to that spike frequency which the ganglion cell sent out in position \vec{r} at time $t - \tau$. Thus with the help of the amacrines the ganglion cell damps its own activity (stabilization of excitation level).

The less compact arrangement of the amacrines justifies us in neglecting spike coincidences. Using a proportionality factor n_2 we introduce the spike frequency of the inhibiting amacrines:

$$(4) \quad \sigma(\vec{r}, t - \tau) = \sum_{i=1}^N \varepsilon \sigma(\vec{r} + \vec{p}_i, t) - \frac{\Theta_0}{2} \sum_{i,j=1}^{N,N-1} \varepsilon^2 \sigma(\vec{r} + \vec{p}_i, t) \cdot \sigma(\vec{r} + \vec{p}_j, t) - \underbrace{n_2 \sigma(\vec{r}, t - \tau)}_{\text{spike frequency of amacrines}}$$

This describes the interaction of the ganglion cells and amacrines. Equation 4 is equally applicable to the network of the on- and off-ganglia. A differentiation occurs only in respect to the stimulus-like activity of the receptor cells. If the receptor cells of the retina are excited, the bipolar cells which are then turned on are induced by the receptor cells to fire spike volleys at the ganglion epithelium, the density of the volleys being analogous to the strength of excitation. Then the ganglion at position \vec{r} may receive in the test interval at point of time t $\sigma_R(\vec{r}, t)$ spikes of the bipolar cells connected with it. If this ganglion cell is of the on-type the spikes will augment the cell's activity. On the other hand the same spikes from bipolar cells have an inhibiting effect for an off-cell. This variable effect of the stimulus-like activity of the bipolar cells we describe thus:

$$(5) \quad \sigma(\vec{r}, t + \tau) = \sum_{i=1}^N \varepsilon \sigma(\vec{r} + \vec{p}_i, t) - \frac{\Theta_0}{2} \sum_{i,j=1}^{N,N-1} \varepsilon^2 \sigma(\vec{r} + \vec{p}_i, t) \cdot \sigma(\vec{r} + \vec{p}_j, t) - n_2 \cdot \sigma(\vec{r}, t - \tau) + \begin{cases} \sigma_R(\vec{r}, t) & \text{for on-cells} \\ - \sigma_R(\vec{r}, t) & \text{for off-cells} \end{cases}$$

We have hereby derived the basic equation of the system model. In the following sections this mathematical formulation will be examined in respect to its consequences.

3. Consequences of the Theory

3.1. Rest Activity of the Ganglion Cells

In numerous investigations of the ganglion epithelium of animal retinas by means of microprobes [2,5,6,7,10] it has been demonstrated, that the ganglion cells, even in the absence of exterior stimuli, show a rest activity of constant spike frequency. This is equally true for both on- and off-cells.

As a first consequence the proposed theory will provide an interpretation of this rest activity. Receptor activity disappears, when no stimuli affect the retina. Thus we set $\sigma_R(\vec{r}, t) = 0$. We then have a spatially homogeneous activity distribution of temporally constant spike frequencies to be assigned. In line with equation 5 their value σ_0 is satisfied by the following:

$$(6) \quad \begin{aligned} \sigma_0 &= \sum_{i=1}^N \epsilon \sigma_0 - \frac{\Theta_0}{2} \sum_{i,j=1}^{N,N-1} \epsilon^2 \sigma_0^2 - n_1 \sigma_0 \\ &= N \epsilon \sigma_0 - \frac{\Theta_0}{2} N(N-1) \epsilon^2 \sigma_0^2 - n_1 \sigma_0 \end{aligned}$$

If we introduce the abbreviations $n_1 = \epsilon N$ and $\Theta = \frac{\Theta_0}{2} N(N-1)$, quantities which are exclusively functions of the system parameters ϵ, N, n_1 and Θ_0 , we obtain as the spike frequency of the rest activity /45

$$(7) \quad \sigma_0 = \frac{1}{\Theta} (n_1 - n_1 - 1) \quad \text{always assuming that } n_1 > n_2 + 1$$

The result is basically a consequence of the spike coincidences. Let us assume, that one ganglion cell has six cells as neighbors (as in Fig. 20), each of which initially sends out one spike per time unit. If a coincidence occurred, the ganglion cell would have to return six spikes to the surround. Each of the neighboring cells (once more presupposing the absence of any spike coincidence) would then activate the cell in question with six spikes at a later moment. All told, for a single unit of time therefore six times six spikes would arrive from the neighboring neurons. Following repeated reflection of the excitation the spike rate would finally have mounted to 6x6x6. That such an explosion-like increase in spike frequency is suppressed is attributable to the fact, that as spike frequency mounts so does the frequency of coincidences and thus likewise more spikes become ineffectual. Finally an equilibrium is reached, in which the statistical spike losses hinder any further increase of spike frequency. Over and above this the amacrine cells as inhibitors contribute their "brake cell" property to the stabilization of this rest level of activity.

3.2. Reproduction of Excitation within the Ganglion Epithelium

The functional properties of the proposed model are presented advantageously, since we are considering the propagation of excitation and inhibition effects around a single neuron subjected to a brief stimulus. This may be realized experimentally by briefly shining a light spot on the dark adapted retina. In Fig. 21 a series of excitation conditions of the ganglion epithelium is represented. These succeed each other at a time interval of the interneuron traveling time τ . Neurons, whose spike frequency momentarily exceeds the rest activity value, are marked in black.

746
747

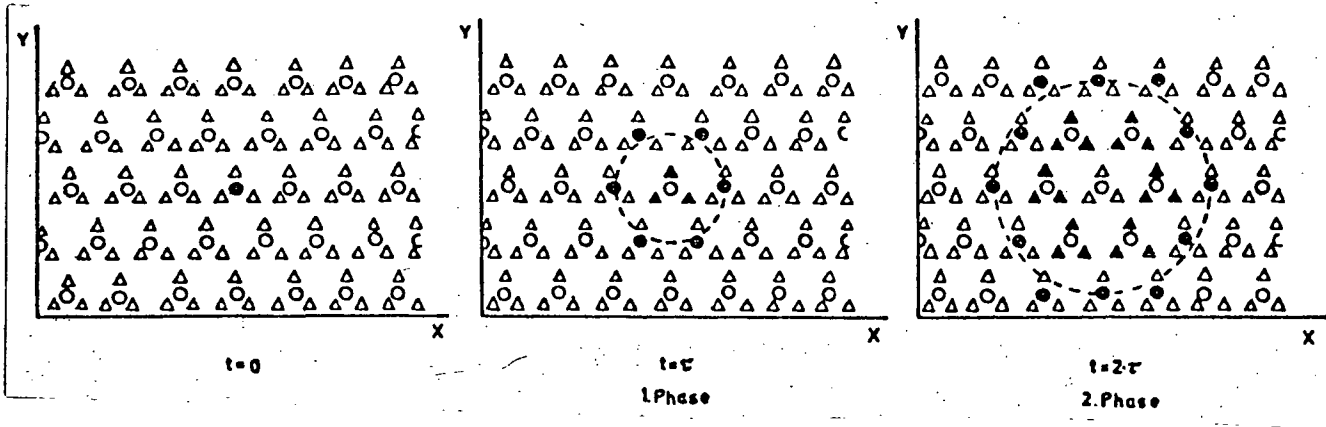


Fig. 21. Phases in propagation of excitation around a ganglion cell. The time interval between two successive phases is τ (interneuron traveling time). Excited neurons (ganglia or amacrine) are in black

At the point in time $t = 0$ the light stimulus increases the activity of a neuron, designated as "source", for a short time above the rest activity level. At time $t = \tau$ the excitation has spread to the adjacent ganglion cells and amacrine, while at the point of source the excitation has once more subsided to the level of rest activity. The stimulated ganglia now activate their surround and would have to reactivate the source ganglion, as we see by means of the second phase in Fig. 21. However the activated amacrine prevent this from happening: their inhibitory spikes meet the stimulating spikes of the surrounding ganglion cells at the source ganglion. At this juncture the source ganglion retains the rest activity value. This means: the shortlived increase in spike frequency for our cell spreads to the surrounding ganglion cells like a ripple. This ripple originates on the one hand from excitation transfer between adjacent neurons and on the other hand from the inhibiting amacrine, which repress any "reflux" of excitation to already activated ganglion cells.

These qualitative considerations should now be complemented by the derivation of a differential equation for stimulus propagation. We stipulate beforehand, that distributions of spike frequencies over the ganglion epithelium, which we describe by means of the position- and time-dependent function $\sigma(\vec{r}, t)$, are to be regarded approximately as constant fields. In such cases we may replace the sums in equation 5 with integrals:

(8)

$$\begin{aligned} \sigma(\vec{r}, t+\tau) &= \frac{n_1}{2\pi} \int_0^{2\pi} \sigma(\vec{r} + \vec{\rho}(\alpha), t) d\alpha - \frac{\Theta}{(2\pi)^2} \iint \sigma(\vec{r} + \vec{\rho}(\alpha), t) \cdot \sigma(\vec{r} + \vec{\rho}(\alpha'), t) d\alpha d\alpha' \\ &- n_2 \sigma(\vec{r}, t-\tau) + \begin{cases} \sigma_R(\vec{r}, t) & \text{for on-cells} \\ -\sigma_R(\vec{r}, t) & \text{for off-cells} \end{cases} \end{aligned}$$

The index vectors $\vec{\rho}_i$ are represented by a vector $\vec{\rho}(\alpha)$, which in integration revolves about an angle α and thus passes through the positions of the vectors $\vec{\rho}_i$. We assure ourselves of the correctness of the selected standardization by inserting the rest activity value. Following a Taylor development of $\sigma(\vec{r} + \vec{\rho}(\alpha), t)$ at point \vec{r} and carrying out of the integrations, the expression in differential form reads:

/48

$$(9) \quad \begin{aligned} \sigma(\vec{r}, t+\tau) &= n_1 \left[1 + \frac{\vec{\rho}^2}{2!} \nabla^2 + \dots \right] \sigma(\vec{r}, t) - \Theta \left\{ \left[1 + \frac{\vec{\rho}^2}{2!} \nabla^2 + \dots \right] \sigma(\vec{r}, t) \right\}^2 \\ &- n_2 \cdot \sigma(\vec{r}, t-\tau) + \begin{cases} \sigma_R(\vec{r}, t) & \text{for on-cells} \\ -\sigma_R(\vec{r}, t) & \text{for off-cells} \end{cases} \end{aligned}$$

In the further calculations higher differential terms than those of the second order are neglected. This is justified in respect to fields, which change very little over the distance between two adjacent ganglia (corresponding to $|\vec{\rho}(\alpha)| \approx 100\mu$).

For the mathematical treatment the quadratic term would prove troublesome. Nevertheless it is possible to find a linear approximation for calculating smaller disturbances. We now set

$$(10) \quad \sigma(\vec{r}, t) = \sigma_0 + \psi(\vec{r}, t)$$

Here the function $\psi(\vec{r}, t)$ describes deviations of the spike frequency for rest activity. Their values would be small in comparison with σ_0 .

A longer transformation of equation 9 following Taylor development of $\psi(t+\tau)$ produces the following differential equation for $\psi(\vec{r}, t)$:

(11)

$$\begin{aligned} \ddot{\psi} + 2 \overbrace{\frac{1-n_1}{1+n_1} \frac{1}{\tau}}^{\delta} \dot{\psi} + \overbrace{\frac{\Theta \sigma_0}{\frac{1}{2}(1+n_1)}}^{\omega_0^2} \psi - \overbrace{\frac{1+n_1 - \frac{n_1}{2}}{\frac{1}{2}(1+n_1)} \frac{\vec{\rho}^2}{\tau^2}}^{c^2} \nabla^2 \psi &= \\ = \frac{1}{\frac{1}{2}(1+n_1)} \begin{cases} \sigma_R(\vec{r}, t) & \text{for on-cells} \\ -\sigma_R(\vec{r}, t) & \text{for off-cells} \end{cases} \end{aligned}$$

The system parameters n_1, n_2, τ, Θ and $|\vec{\rho}|$ are now introduced into the new, positively defined system constants δ, ω_0 and c . This is the differential equation for the propagation of damped waves (telegraph equation). As one might already expect on the basis of the preceding considerations of plausi-

bility, the dissemination velocity of these waves is determined by the parameters $|\bar{\rho}|$ and τ . One should estimate the value of $|\bar{\rho}|$ at some 100 microns [11] and that of τ at 1 msec (synaptic lag). Thus for the velocity of the excitation waves we have to expect a value on the order of $10 \frac{\text{cm}}{\text{sec}}$. In a later section we will come back to a procedure for determining this velocity.

At first blush the reader might be biased against the theory by the fact, that the spike volleys produced under receptor excitation by a ganglion may also induce neurons in the surround to send out spikes. A qualitative look at the picture might incline one to think, that the functional structure of the retina was so ordered, that it would control the excitation generated by a light spot in the retinal layers by restricting the excitation to the area of a ganglion-neuron. This is true of course for the center of the retina. For peripheral portions of the retina, which moreover do not exhibit any great amount of definition, we do not need to pursue the above argument. The fact that on the contrary the wavelike diffusion of the excitations specifically may have a "biological meaning", should be demonstrated by a consideration of the excitation diffusion which a moving point of light produces in the ganglion epithelium in line with the present model. The considerations are developed with the help of Fig. 22.

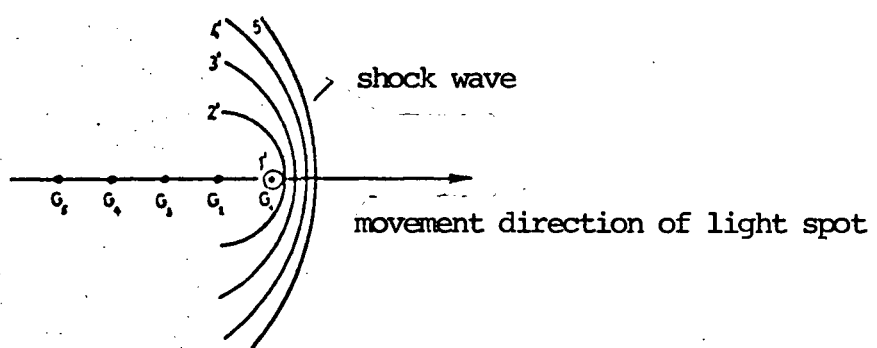


Fig. 22. Buildup of a shock wave with moving excitation point

Let a point of light be moving at constant velocity over the retina. At moment t it sweeps over the ganglion cell 1, whereupon the latter begins to set up a ripple 1'. Meanwhile at a point in time, which is Δt earlier, the point of light had illuminated cell 2 and released from it a ripple, which at the time of our consideration had spread to circle 2'. If the velocity of excitation propagation is represented by c , this circle has a radius of $c \cdot \Delta t$. The other ripples, 3', 4', etc., left ganglion cells 3, 4, etc., swept by the point of light, at a correspondingly earlier time. Fig. 3 shows that there is a concentration of stimulus waves in the direction of the light point's movement, while the ripples in the direction opposite to that of the velocity vector seem to be shoved apart (Doppler effect). The concentration of the excitation after the fashion of a "shock wave" has as a consequence, that the spike frequency is pre-increased precisely for those ganglion cells, which are likely to be affected the next moment by the spot of light. The shock wave preceding the light spot is responsible for the fact, that the light impinges upon a pre-activated ganglion cells and in this way it can reinforce the sti-

mulation effect of the light.

The "biological meaning" of the proposed model is revealed even more clearly, when we recapitulate the considerations from an information theory point of view.

3.3. Informational Theory Aspect of the System Model

We may regard as an information source a ganglion cell, which at every point in time makes a selection between two signals, spike and pause. Thus the ganglion cell has at its disposal an alphabet with the two letters S (spike) and P (pause). Every piece of information communicated to the brain by means of the cell's optic nerve fibers has approximately the following form: SPSSPPSSPPSPSP. The information value of the two signs is a function of the probability of their occurrence. (Shannon, Weaver, Wiener). It is easy to derive relationships for these probabilities from our theory: the maximal spike frequency of which a ganglion cell is capable is determined by the reciprocal refractory time (dead time). Thus there must be a connection between the spike frequency σ and the pause frequency π through the relation

/51

$$(12) \quad \sigma + \pi = \frac{1}{\Theta_0}$$

Accordingly the probabilities for the occurrence of spikes and pauses are represented by the products $\sigma \cdot \Theta_0$ and $\pi \cdot \Theta_0$.

Let us now consider, in contrast to the proposed model, a collection of ganglions, where the cells show rest activity with frequency σ_0 , but are incapable of setting up any excitation waves. According to the Shannon formula [12] the occurrence of spike and pause has the following information values:

$$(13) \quad \begin{aligned} I_{\text{Spike}} &= - \text{ld} (\sigma_0 \cdot \Theta_0) && \text{ld} = \text{Log. dualis} \\ I_{\text{Pause}} &= - \text{ld} (\pi_0 \cdot \Theta_0) = - \text{ld} (1 - \sigma_0 \cdot \Theta_0) \end{aligned}$$

At a point in time t a moving spot of light would sweep over one of the on-ganglia with the result that the latter would experience a weight displacement between spike and pause probabilities in favor of the spike, while the brain is still expecting these signs with the original probabilities $\sigma_0 \cdot \Theta_0$ and $\pi_0 \cdot \Theta_0$. Thus the average information that would have to be processed by the brain during apperception would amount to

$$(14) \quad \bar{I}_1 = - \text{ld} \sigma_0 \cdot \Theta_0 \cdot (\sigma_0 + \sigma_1) \cdot \Theta_0 - \text{ld} (1 + \sigma_0 \cdot \Theta_0) \cdot (1 - (\pi_0 + \pi_1) \cdot \Theta_0)$$

probabilities for spike and pause at moment of light excitation

information values for spike and pause

Let us turn once more to the proposed model

/52

At the moment in time t when the point of light sweeps over the ganglion in question the impulse rate is increased as before by the receptor impulse frequency. However the shock wave preceding the light spot had already raised the

spike frequency of the ganglion at an earlier point in time. Herewith the brain received a "forewarning" so that the anticipated probability went up from σ_0 to $\sigma_0 + \psi$. The average amount of information to be processed by the brain in this case is

(15)

$$\bar{I}_2 = - \underbrace{[d(\sigma_0 + \psi)\theta_0 \cdot (\sigma_0 + \sigma_R)\theta_0]}_{\text{information values for spike and pause according to the proposed model}} - \underbrace{[d[1 - (\sigma_0 + \psi)\theta_0][1 - (\sigma_0 + \sigma_R)\theta_0]]}_{\text{information values for spike and pause according to the proposed model}}$$

information values for spike and pause according to the proposed model

As is shown in textbooks on information theory [e.g. 3,4,12] the average amount of information is smaller in proportion the closer the expected probabilities of any signals whatsoever, come to their actual frequencies (informational accommodation). As shown by a comparison of equation 14 with equation 15, this is the case with the proposed model.

3.4. Spike Histograms of the Ganglion Cells with Allowance for Temporal Excitation Gradients

In this section we will examine the phasic reaction patterns of ganglion cells to test stimuli, whose intensity is evenly distributed to the surface elements of the retina (as might be the case when looking at a homogeneous surface) and therefore presents an exclusive time dependence.

Equation 11, by means of which we can calculate deviations of neuron frequency from the level value of rest activity, is simplified in this case thus:

(16)

$$\ddot{\psi}(t) + 2\delta \dot{\psi}(t) + \omega_0^2 \psi(t) = \frac{1}{\xi^2(1+x_1)} \cdot \sigma_R(t)$$

The Fourier transformation then yields for each temporal excitation gradient of receptor activity $\sigma_R(t)$ the corresponding temporal function $\psi(t)$. Fig. 23 juxtaposes results for two test stimuli (flash of light and rectangular pulse). System parameters were $\delta = 3 \cdot 10 \text{ sec}^{-1}$ and $\omega_0^2 = 3 \cdot 10^3 \cdot \text{sec}^{-2}$.

/53

The phasic reaction patterns obtained by the theory reproduce the course of ganglion cell reaction patterns obtained from animal retinas using microprobes [5,10].

3.5. Transfer Characteristic of Ganglion Epithelium in respect to Alternating Current Excitation

/54

We are convinced, that it is permissible to treat the ganglion epithelium as a circular disc, which we conceive as evenly populated by ganglion cells and amacrine cells. This idealization may be justified by the fact, that the nerve interactions of the retinal neurons function independently of the topological configuration of the retina. Let us then suppose that our discoid epithelium is exposed to a temporally periodic excitation field in such a way, that each neuron of the ganglion layer experiences stimuli of the same strength. Then

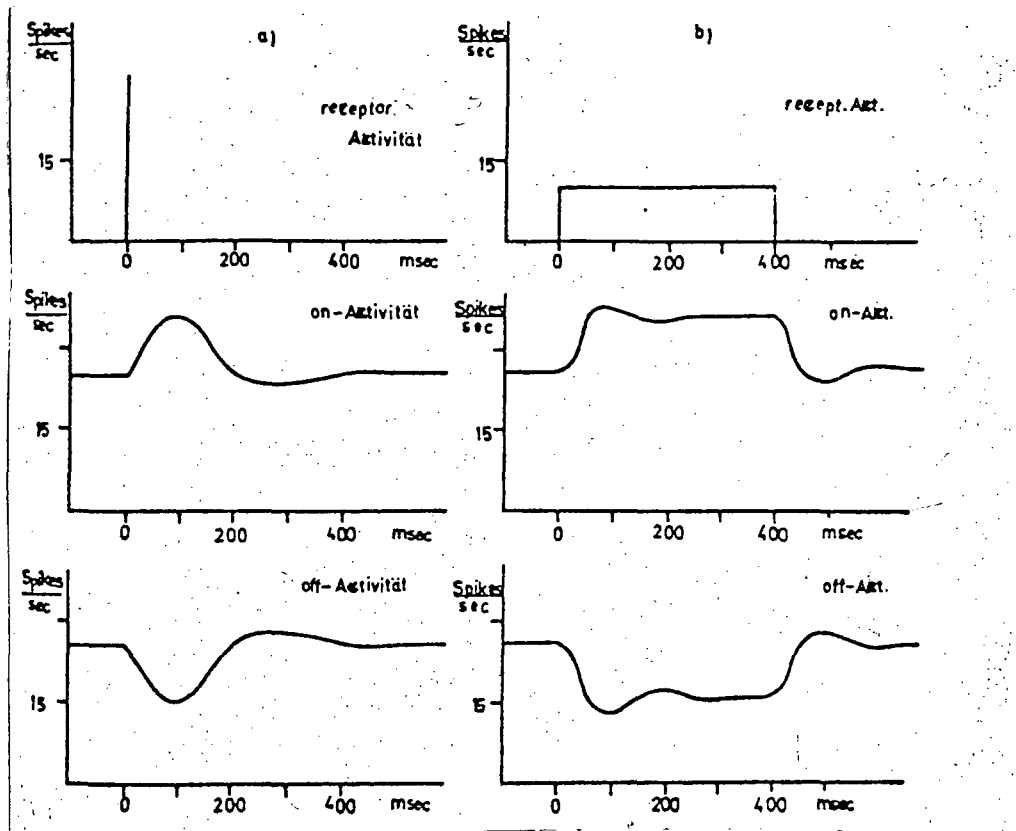


Fig. 23. Spike histograms of on- and off-ganglia for temporal excitation gradients: a - flash of light, b - rectangular pulse

the alternating excitation field modulates, at its frequency f , the impulses of the on- and off-ganglia. Naturally, the activity modulations of the off-cells are contraphase to those of the on-ganglia. Inasmuch as the interneuron interaction overlaps the effect of the alternating stimulus current in a facilitating or damping way, it determines in what relationship the intensity of the excitation pulses are translated into neuron impulse volleys. This transfer ratio will thus change as a function of the series frequency of the excitation pulses. The following lines of thought will furnish us with mathematical relationships for describing this transfer property.

If the cells of the ganglion epithelium did not engage in interaction, the alternating stimulus would, at every part of the retina, have the effect of synchronous modulations of the spike volleys for on- and off-ganglia. If we picture the interaction of the ganglion cells and amacrines as going on, each ganglion has the ability, already described, to communicate its own excitation to the surround in the form of successive ripples. Thus each ganglion may be looked upon as a center of Huygens waves. Then through the interference of the ripples emanating from the individual cells definite distributions of activity are set up within the ganglion epithelium. To illustrate this let us consider any circle around the midpoint of the epithelium (Fig.24).

Under the alternating stimulation each cell of this circle emits Huygens wavelets. Thus two wave fronts are set up, the one going towards the edge of the retina and the other contracting around the center. At the moment when

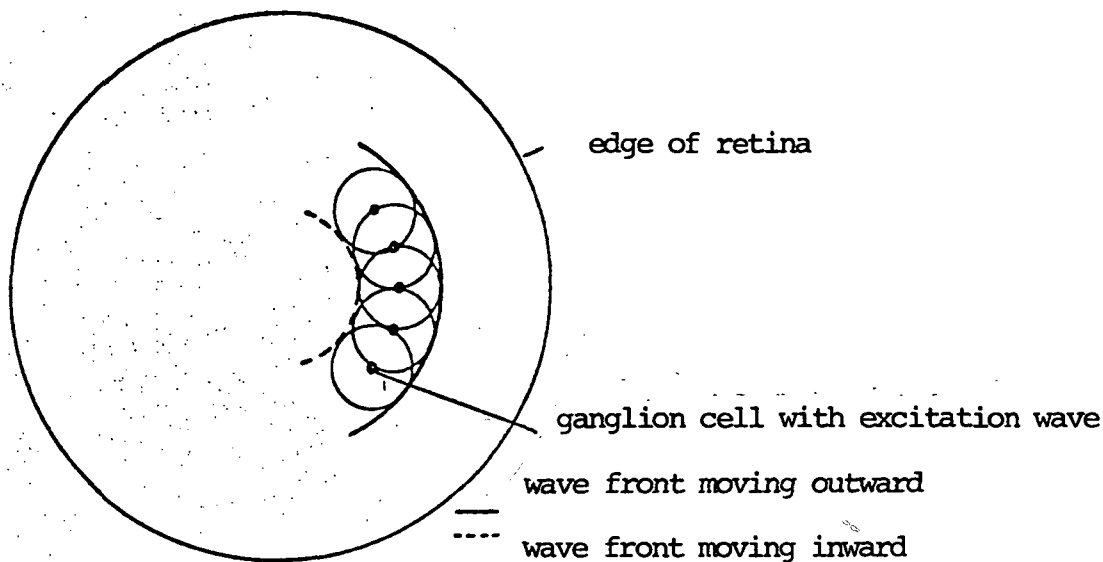


Fig. 24. Formation of concentric ripples within the ganglion epithelium

one of the outward bound wave fronts reaches the edge it excites the ganglion cells situated there. This causes them likewise to become Huygens centers and to send a wave front to the interior of the epithelium. This means, that the excitation waves reaching the edge are reflected there cophasically. The same mechanism also brings it about, that the inward bound wave fronts are reflected at the center.

We may picture further concentric circles between the center and the edge, from which inward and outward bound waves are released, so that finally the entire wave field may be regarded as an overlapping of such ripples. Their wavelength λ is related to the frequency of the stimulus f in the elementary ratio

/56

$$(17) \quad \lambda = \frac{c}{f}$$

wherein c represents the wave velocity constant.

By interference these waves can cancel each other out more or less effectively. However for specific values of the excitation frequency f they use constructive interference to set up stationary wave fields. The condition for constructive interference is satisfied, when at every point in time the crests of outbound wave trains coincide with those of inbound ones.

Fig. 25 presents moment diagrams of the inbound and outbound wave trains at the moment, when the spike frequency for the ganglion cells of the center is at its exact maximum. Because of cophasic reflection at the edge of the retina the reflected wave trains coincide with the outbound ones, whenever a multiple of the half-wavelength matches the radius R of the retina. This implies the condition, that in cases of constructive interference an oscillation loop always comes to rest on the edge of the retina. Expressed in formula form the condition for constructive interference reads:

/57

$$(18) \quad \frac{\lambda}{2} \cdot n = R$$

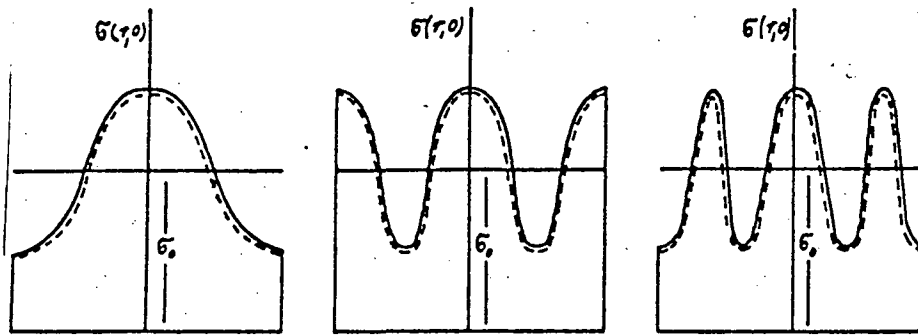


Fig. 25. Moment diagrams of inbound and outbound excitation waves in three cases of constructive interference

If we express λ in terms of its frequency dependence (equation 17), we obtain the following values for the stimulation frequencies:

$$(19) \quad f = \frac{c}{2R} \cdot n$$

Thus stationary wave fields are set up only for whole multiples of a basic frequency expressed by $c/2R$. If stimulations are applied at other frequencies, the excitation waves cancel each other out everywhere within the ganglion epithelium.

Following these direction-finding plausibility considerations we should take up the problem of the periodic stimulation of a circular, homogeneous ganglion assembly mathematically, i.e. by integration of equation 11. There is no possibility of a closed solution of the damped system. On the other hand the solutions for the non-damped system are easily attained. Since they will be very useful in our further considerations, differential equation 11 will be treated while neglecting the damping term ($\delta = 0$).

3.5.1. The Non-damped System

Let each ganglion be engaged by a temporally periodic excitation intensity in such a way, that each ganglion cell receives from its appropriate receptors fluctuating rates of receptor impulses in the rhythm of the excitation frequency f . The time dependence should be cosinusoidal. The amplitude of the stimulus-like receptor activity would be the same A_0 in every part of the retina. Setting $\delta = 0$ the differential equation for $\psi(\vec{r}, t)$ would read

$$(20) \quad \ddot{\psi}(\vec{r}, t) - c^2 \nabla^2 \psi(\vec{r}, t) = \frac{1}{\sum_i (1+n_i)} A_0 \cos 2\pi f t = A \cos 2\pi f t$$

The Laplace operator ∇^2 needs merely to be developed for this problem according to a polar coordinate and reads

$$\nabla^2 = \frac{\partial^2}{\partial r^2} + \frac{1}{r} \frac{\partial}{\partial r}$$

To this differential equation we must then add the boundary condition, according to which the amplitude of activity oscillation $\psi(\vec{r}, t)$ at the edge of the ganglion epithelium must have a maximum, so that

$$|\psi(R, 0)| = \text{Maximum.}$$

The alternating excitation intensity will provide the time dependence for the required solution. Therefore we attempt the integration of differential equation 20 with the following separation formula:

$$(21) \quad \psi(r, t) = a_k \cdot J_0(kr) \cdot \cos 2\pi f t$$

It will prove advantageous to represent position dependence by the Bessel function $J_0(kr)$ [13]. a_k describes the amplitude strength of the activity pattern stimulated by the mutual excitation. We insert the assumed solution, equation 21, into differential equation 20 and by applying the orthogonality relations for Bessel functions [13] obtain the following relationship:

$$(22) \quad \left\{ -(2\pi f)^2 - c^2 k^2 - \omega_0^2 \right\} a_k \cdot \frac{R^2}{2} [J_0(kR)]^2 = A \frac{R}{k} J_1(kR)$$

By choosing specific values k_n for the parameter k the required boundary condition may be satisfied:

$$(23) \quad \left[J_0(k_n R) \right] = \text{Max.} \quad \text{or} \quad \left. \frac{\partial}{\partial r} J_0(k_n r) \right|_{r=R} = -J_1(k_n R) = 0$$

It then follows from equations 22 and 23, that only for specific values of the excitation frequency f do amplitude factors a_{k_n} other than zero exist. The calculation is made by the following passages to limit:

$$(24) \quad a_{k_n} = \lim_{k \rightarrow k_n} a_k \left|_{2\pi f = \sqrt{c^2 k^2 + \omega_0^2}} = \frac{AR}{c^2 (k_n R)^2 J_0(k_n R)} \quad \text{/59}$$

Finally for the spatiotemporal distribution of the impulse frequency $\sigma(r, t)$ the following applies

$$(25) \quad \sigma(r, t) = \sigma_0 + \psi(r, t) = \begin{cases} \sigma_0 & \text{für } f = \frac{\sqrt{c^2 k_n^2 + \omega_0^2}}{2\pi} \\ \sigma_0 + \frac{A}{c^2 k_n^2 J_0(k_n R)} J_0(k_n r) \cdot \cos 2\pi f t & \text{für } f = \frac{\sqrt{c^2 k_n^2 + \omega_0^2}}{2\pi} \end{cases}$$

Two consequences of these results should be brought out:

a) Discrete Excitation Frequencies

Although the alternating stimulus therefore engages each point of

the ganglion epithelium with equal intensity, it is capable of stimulating in the ganglion epithelium spatially structured excitation patterns. In any case the temporal periodicity must agree with a discrete frequency value

(26)

$$f_n = \frac{1}{2\pi} \sqrt{c^2 k_n^2 + \omega_0^2}$$

They represent natural frequencies of the ganglion assembly. As is shown in pertinent textbooks, for those arguments, $k_n R$, of the Bessel function $J_0(k_n R)$ which satisfy equation 23, the following is approximately true

(27)

$$k_n R \cong \pi \cdot n$$

If ω_0^2 has a negligible value, the result of (26) and (27) will be that, which we already derived on the basis of plausibility considerations (see equation 19).

b) Average Intensity of the Excitation Pattern

/60

A qualitative picture of the activity patterns is presented by their nodal lines. That means those places in the ganglion epithelium where the excitation waves of the ganglion cells interfere in such a way, that deviations of impulse frequency from the rest activity level are excluded. Fig. 26b shows such nodal lines for the first activity patterns. The impulse frequency of all those cells, which find themselves between these nodal lines, fluctuates in the rhythm of the excitation field around the rest activity value. We are interested in the intensity at which excitation patterns appear at a predetermined amplitude of the excitation strength of the alternating excitation field. For this purpose there is a criterion in the oscillation amplitude, communicated to the entire retina, of the spike frequency. First of all we find the square of the locally variant amplitude over the entire surface of the retina:

(28)

$$\frac{1}{\pi R^2} 2\pi \int_{r=0}^R [\psi(r,0)]^2 r dr = \frac{2}{R^2} \int_{r=0}^R a_n^2 [J_0(k_n r)]^2 r dr = \frac{A^2}{[c^2 k_n^2]^2} = \frac{A^2}{[(2\pi f_n)^2 - \omega_0^2]^2}$$

We define the root of this value as the measure for the average excitation amplitude of the corresponding activity pattern.

(29)

$$\bar{\psi} = \frac{A}{(2\pi f_n)^2 - \omega_0^2}$$

Thus at constant excitation amplitude A the excitation patterns for the higher stimulation frequencies become increasingly harder to recognize. In Fig. 26a there is a representation of the frequency dependence of the average excitation intensity for the individual excitation patterns.

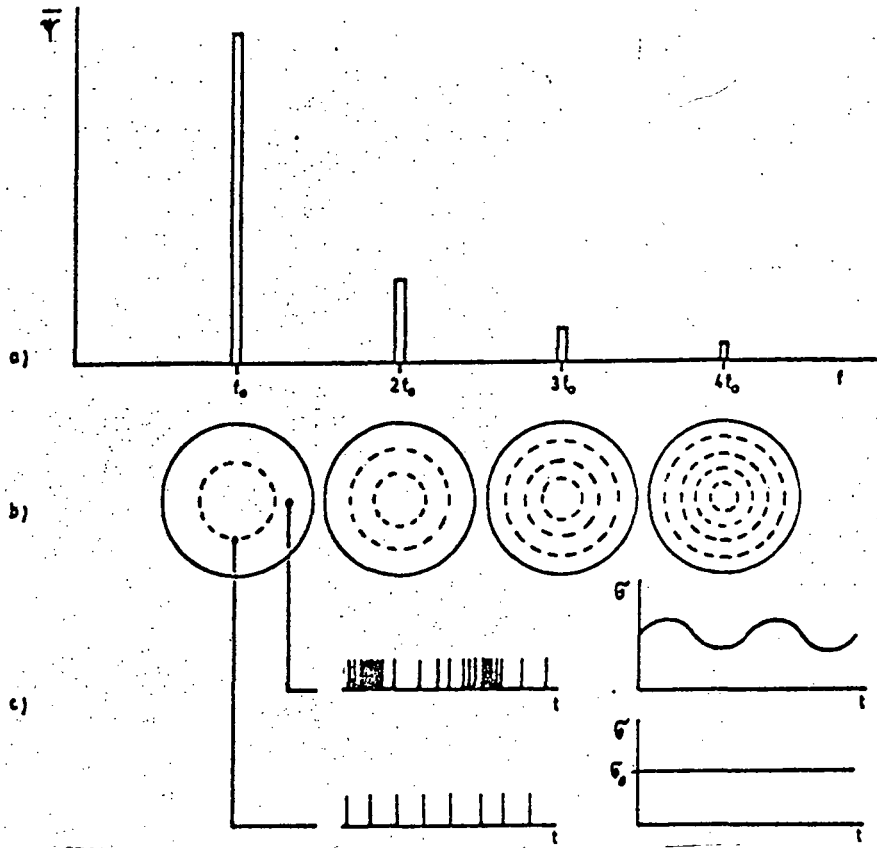


Fig. 26. Spectrum of the first four excitation patterns: a - average fluctuation amplitude of spike frequency as a function of excitation frequency, b - excitation pattern structures brought out by nodular lines of spike fluctuations (broken lines of circles), c - spike histograms taken at various places in the first excitation pattern

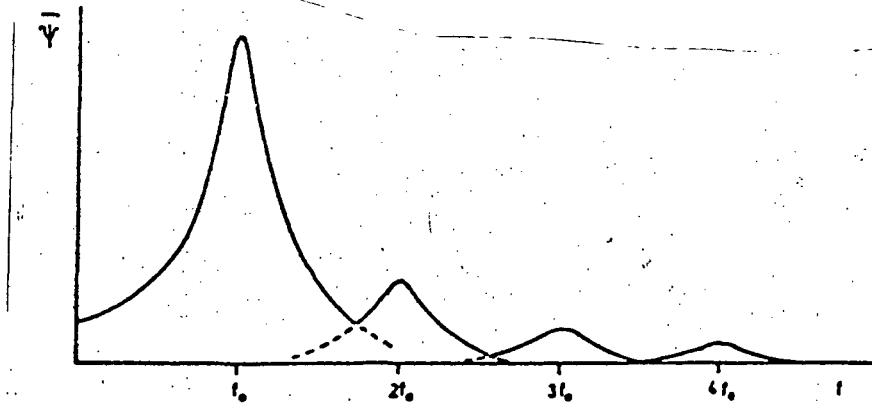


Fig. 27. Frequency dependence of average spike fluctuation with weak damping of excitation waves

3.5.2. The Damped System

We will attempt likewise approximately to find the average amplitude $\bar{\Psi}$ for

the surround of one of the discrete resonance frequencies f_n . The damping constant δ would now be small (weak damping) although larger than zero. We describe the alternating excitation effect by the complex phase $\exp i 2\pi f t$. Then the following inhomogeneous differential equation is the basis for the damped wave dispersion:

$$(30) \quad \ddot{\psi} + 2\delta\dot{\psi} + \omega_0^2\psi - c^2\nabla^2\psi = \begin{cases} A e^{i2\pi f t} & \text{for } 0 \leq r \leq R \\ 0 & \text{otherwise} \end{cases}$$

We are looking for solutions of the type:

$$(31) \quad \psi(r,t) = a(f) \cdot J_0(kr) \cdot e^{i2\pi f t}$$

This assumed solution is inserted into equation 30. By means of the orthogonality relations for Bessel functions [13] we finally arrive at the complex excitation amplitude $a(f)$:

$$(32) \quad a(f) = \frac{A \cdot J_1(kR)}{\frac{1}{2} k \cdot J_0^2(kR)} \frac{1}{(2\pi)^2 [f_n^2 - f^2 + i \frac{\delta}{2\pi} f]}$$

We average now the square of the position-dependent amplitude $\psi(r,0)$ over the whole excitation pattern:

$$(33) \quad \frac{2\pi}{\pi R^2} \int_0^R |\psi(r,0)|^2 r dr = \frac{2}{R^2} |a(f)|^2 \int_0^R J_0^2(kr) r dr = \left[\frac{A J_1(kR)}{\frac{1}{2} J_0(kR)} \right]^2 \frac{1}{|f_n^2 - f^2 + i \frac{\delta}{2\pi} f|^2}$$

We had already defined the root of this expression at another place as the measure for the average excitation amplitude .

$$(34) \quad \bar{\psi} = \frac{A |J_1(kR)|}{\frac{1}{2} |J_0(kR)|} \frac{1}{\sqrt{(f^2 - f_n^2)^2 + (\frac{\delta}{2\pi} f)^2}}$$

In the passage to limit $\delta \rightarrow 0$ this expression, provided we still satisfy the required boundary conditions, is transformed to the relationship given in equation 29. Therefore for small values of δ we may envisage the following approximation:

/63

$$(35) \quad \bar{\psi} = \frac{A}{(2\pi f_n)^2 - \omega_0^2} \frac{\frac{\delta}{2\pi} \cdot f_n}{\sqrt{(f^2 - f_n^2)^2 + (\frac{\delta}{2\pi} f_n)^2}}$$

If in the case of a non-damped propagation of the excitation waves we had gotten sharp spectral lines (see Fig. 26a), the damping would have led to a final line width. Fig. 27 shows the frequency dependence of the average fluctuation amplitudes of the damped system.

3.6. Theoretical Interpretation of the Flicker Threshold Process

The consequences just drawn from the proposed theory can be translated into the results that we had gotten in investigating the test subjects of our control group.

The average amplitude $\bar{\Psi}$ shows how much the spike frequency (averaged over one of the possible patterns) fluctuates around the rest activity value. However the intensity of the subjective flicker impression of a test subject must be viewed in correlation to this amount of fluctuation of the retinal spike frequency. For an interpretation of the flicker threshold process we need merely require, that the average fluctuation amplitude $\bar{\Psi}$ of an excitation pattern be transposed to subjective flickering the moment this amplitude exceeds a certain minimum value. This kind of threshold value must be assumed on the grounds that the statistical fluctuations of rest activity necessarily lead to subjective flickering on a regular basis in case of failure on the part of this threshold.

In detail the theoretical foundation of the properties of the flicker threshold curve reads as follows:

/64

a) Harmonious Minimum Frequencies

In accordance with the theory an alternating stimulus is capable of producing an excitation pattern in the ganglion epithelium only when its frequency f takes on one of the discrete values f_n . The reason is that only for these frequencies is there constructive interference of the excitation waves within the ganglion epithelium. Naturally, in this form the theory is an idealization. (We began by neglecting the effect of damping of excitation waves) Nevertheless the theory illustrates the principle, according to which subjective flickering may be aroused for specific values of the excitation frequency in a preferential way. The direction taken by a realistic description of the relationships would be, that a stimulation of retinal activity patterns is also possible at other frequencies, but then there would be a requirement of help from a corresponding increase in the excitation amplitude A_0 . Thus on either side of one of the discrete excitation frequencies the stimulus strength must be increased, if a recognizable excitation pattern is to emerge. However the values of the excitation frequency are approximately whole multiples of a basic frequency f_0 (see equation 19). In this way we have drawn attention to the most striking finding in respect to frequency dependence of the flicker threshold.

Since we know the values for the minimum frequencies from measurements of the flicker threshold curves and may set as a basis an average value of about 2cm for the radius of the retina [8], equation 19 permits us to further define the diffusion velocity of the excitation waves. The first minimum ($n=1$) for the flicker threshold curves of our control group often occurs around 7 Hz.

Thus from equation 19 we have the following value for the velocity of excitation diffusion: $c = 7 \text{ sec}^{-1} \cdot 2 \cdot 2 \text{ cm} = 28 \frac{\text{cm}}{\text{sec}}$.

We had already estimated the magnitude of the velocity constant c in a previous section using the values of the interneuron traveling time of a nerve impulse and the average distance between adjacent ganglion cells. Thus the measurements confirm the theoretically derived magnitudes for the system parameter c . /65

b) Tentential Course of the Flicker Threshold

The onset of subjective flicker can be observed by the test subject as soon as the average fluctuation intensity Ψ of an excitation pattern has attained a threshold value of $\Psi_{\text{threshold}}$. Between the smallest excitation amplitudes A , which are sufficient for stimulating a subjective flicker, and the corresponding frequencies f_n the following relationship exists

$$(36) \quad A = \Psi_{\text{threshold}} \left[(2\pi f_n)^2 - \omega_0^2 \right]$$

Now in order to be able to interpret the stimulation of a subjective flicker by means of an electric alternating current, one would have to know the way in which the electric current density j is translated into the corresponding impulse frequency of the excitation amplitude A . This would be done largely through the linear relation

$$(37) \quad A \sim \begin{cases} j - j_{\text{Rheobase}} & \text{f\u00f6r } j > j_{\text{Rheobase}} \\ 0 & \text{f\u00f6r } j < j_{\text{Rheobase}} \end{cases}$$

This states, that a threshold current (rheobase) is also required for stimulation of an individual neuron. If the current density is in excess of the rheobase value, the overlap is proportionally translated by the impulse frequency of the neuron. Presupposing ohmic behavior of the resistance system electrode-body-electrode, the current density j will be proportional to the voltage U of the electric excitation pulses. /66

$$(38) \quad A \sim \begin{cases} U - U_{\text{Rheobase}} & \text{f\u00f6r } U > U_{\text{Rheobase}} \\ 0 & \text{f\u00f6r } U < U_{\text{Rheobase}} \end{cases}$$

Neglecting the system parameter ω_0^2 already shown to be small, we get from equations 36 and 38 the following frequency dependence of threshold voltages for subjective flicker:

$$(39) \quad U = U_{\text{Rheobase}} + \text{const. } f_n^2$$

The relationship given by equation 39 can be very clearly demonstrated by the test record of subjects M.A. and M.H.. In Figures 28 and 29 the minimum frequencies for these subjects are plotted on a quadratic scale. Together with the ordinate values of the threshold voltages they define points of measurement, which lie along straight lines within the limits of error, as would be expected on the basis of the equation 29 relationship.

The steady rise of threshold voltage with the square of the excitation frequency may also be demonstrated for test subjects N.R. and Sch.W. (from the control group), as we know from Figures 30 and 31. Deviations from the theoretically derived relationship do occur, however, at small excitation frequencies. For these lower excitation frequencies the threshold voltages are higher, as we would expect on the basis of theoretical considerations. However this discrepancy between theory and measurement disappears, if we take a further look at the polarization capacity of human tissue. The tissue between the two excitation electrodes sets up against the alternating currents not only ohmic resistance but also a capacitive resistance component. If we represent the ohmic resistance of the system electrode-tissue-electrode by R and capacity by C , we must alter the simple proportionality between voltage and current density as follows:

/67

(40)

$$j \sim \frac{u}{\sqrt{R^2 + \left(\frac{1}{2\pi C f}\right)^2}}$$

Thus, since there is increased total resistance for alternating currents of lower frequency, we must increase the corresponding voltage values in order to attain once more a current density j at a threshold strength capable of stimulating the neurons. As can be easily verified, the consideration of the polarization capacity results in the following correction of the relationship given in equation 39:

(41)

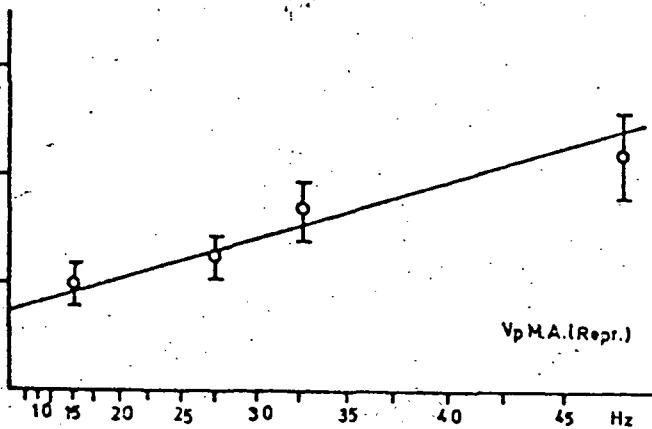
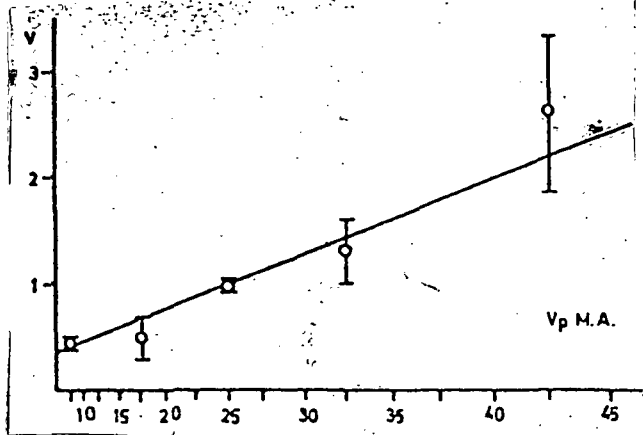
$$u = (U_{\text{rheobase}} + \text{const. } f_n^2) \sqrt{1 + \frac{1}{(2\pi RC)^2 \cdot f_n^2}}$$

Thus we also obtain a theoretical explanation for the fact that for many test subjects there is also a slight rise in the tendential curve of the frequency dependent threshold in the case of small excitation frequencies.

c) The Threshold Curve

/70

The arguments about the frequency behavior of average excitation amplitudes when damping does not disappear may be considered as approximate to a resonance-frequency for calculation of the flicker threshold. We satisfy the threshold condition, inasmuch as we set the average amplitude obtained by equation 35, ψ , as equal to $\psi_{\text{threshold}}$ and take account of the proportionality between the excitation amplitude A and the stimulation voltage U . Thereby we obtain for a surround of a resonance frequency the following frequency dependence of the minimal excitation voltage:



/68

Fig. 28. Voltage- f^2 diagrams for test subject M.A.

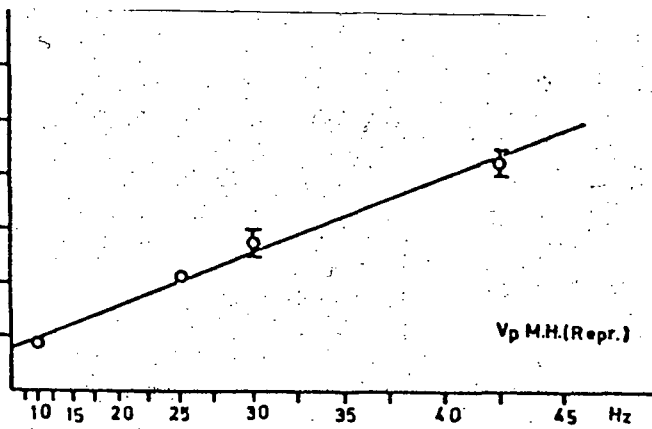
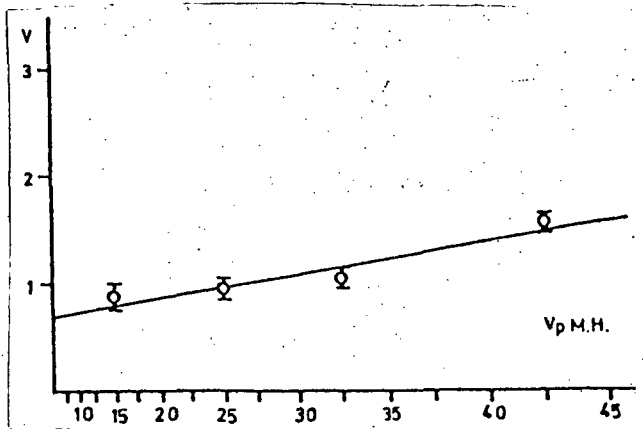
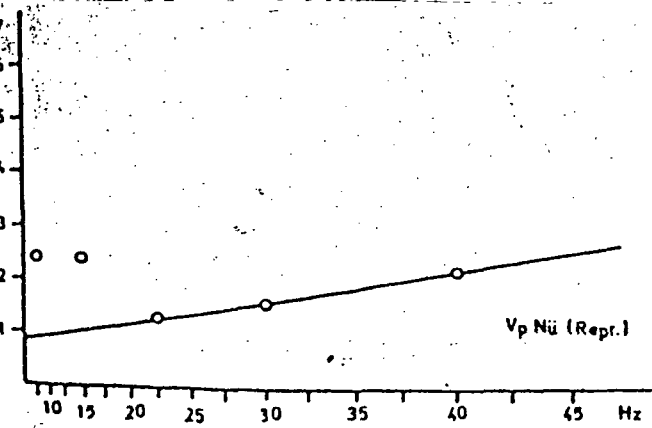
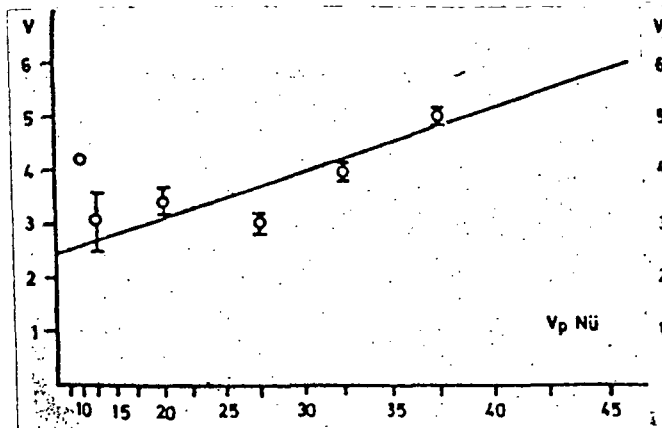


Fig. 29. Voltage- f^2 diagrams for test subject M.H.



/69

Fig. 30. Voltage- f^2 diagrams for test subject Nü

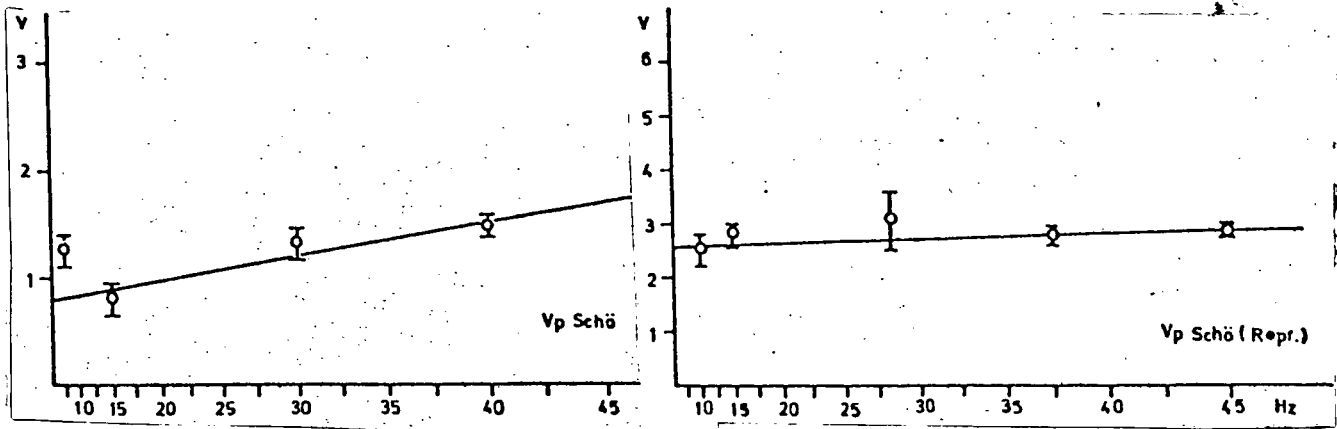


Fig. 31. Voltage- f^2 diagrams for test subject Schö.

(42)

$$U = U_{\text{rheobase}} + \text{const. } f_n^2 \cdot \frac{\sqrt{[f^2 - f_n^2]^2 + \left(\frac{\delta}{2\pi} f_n\right)^2}}{\frac{\delta}{2\pi} f_n}$$

/70

The constants U_{rheobase} , const. and δ were matched with the record of a member of the control group (M.H. Repr.). Fig. 33 shows the degree of agreement between the theoretically and experimentally obtained course of curves.

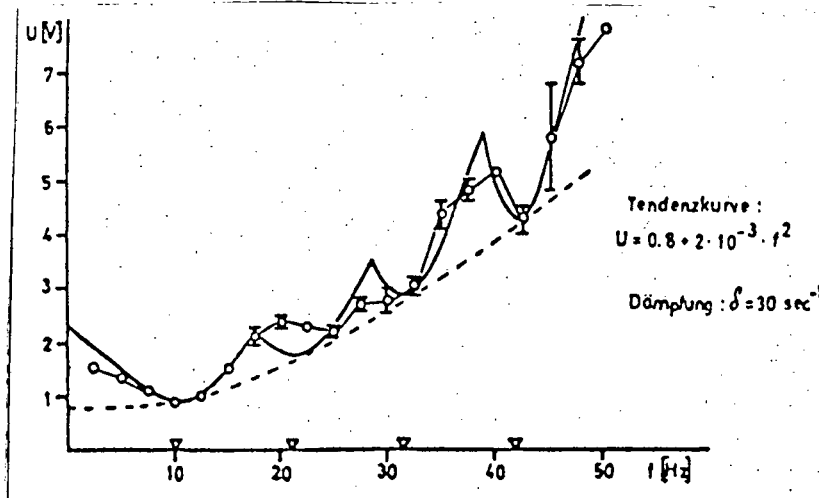


Fig. 33. Comparison of theoretical and experimental flicker threshold curve (of test subject M.H.).
Tendenzkurve: tendential curve; dämpfung: damping.

3.7. Effect of Pathological Changes in the Retina on the Course of the Flicker Threshold /71

The theory makes it possible to explain a number of striking findings that resulted from investigation of patients with pathologically modified retinas.

a) Injury to Global Receptor Epithelium

We must begin with the fact, that the excitation currents stimulate all layers of the retina to the same degree. The ganglion layer of a healthy retina therefore perceives an amount of stimulation composed of two parts: the excitation which the electric current delivers to the ganglion cell by its direct effect and the supplement excitation produced by the volley discharges of the receptors and bipolar cells that are stimulated likewise. If then the receptor layer is totally absent, the ganglion cells are only deprived of the innervating contribution of the receptors. In other respects the effect of the current on the ganglia is the same as before. This explains, why we do not observe any changes in discrete excitation frequencies nor modifications of the tendential course of the flicker threshold curve (see Fig. 9a-d). This becomes more apparent, if we again plot the threshold voltages against the squares of the excitation frequencies. Our patients with total impairment of the receptor epithelium satisfy, as Fig. 34a-d shows, the relationship set up by equation 39.

b) Injury to Central Areas of Receptor Epithelium

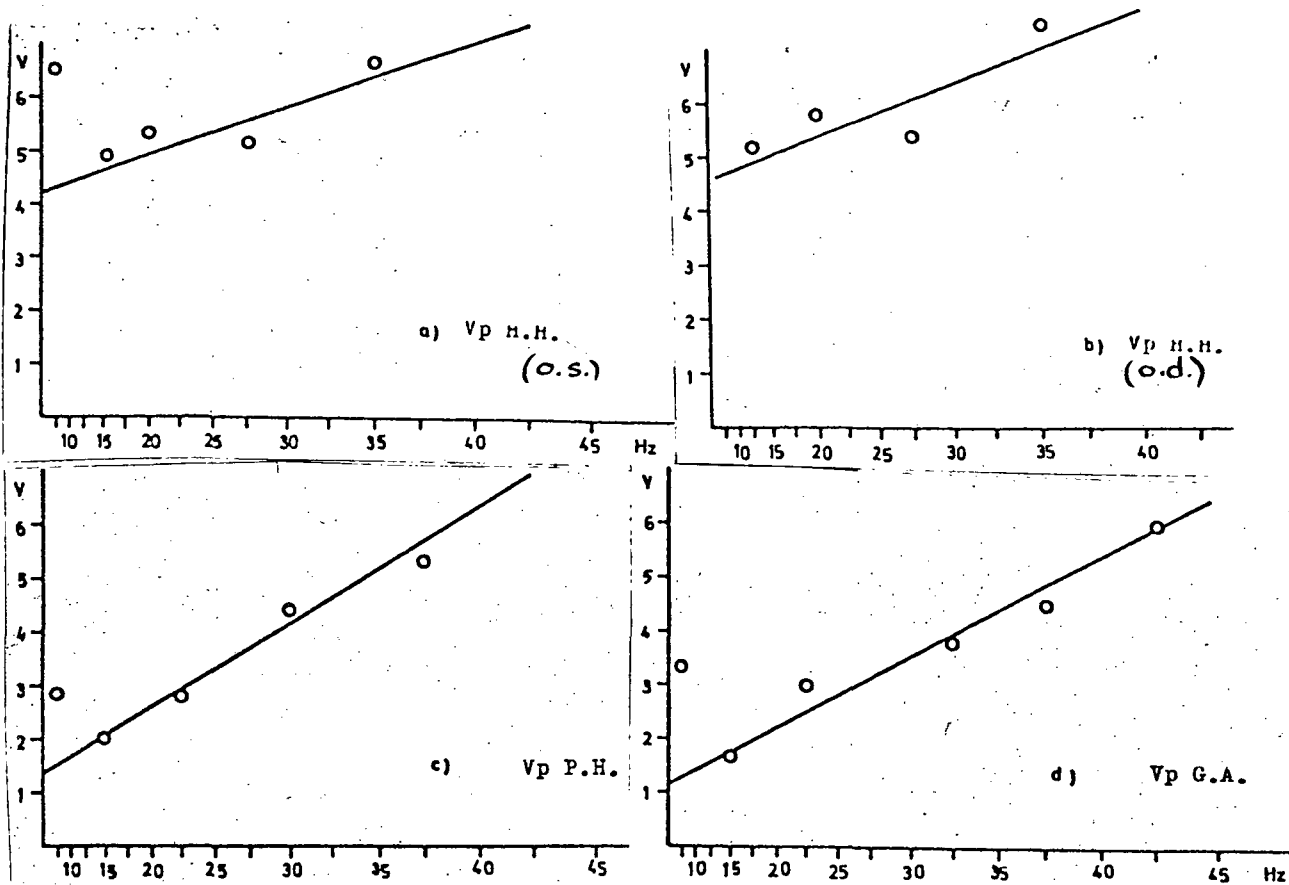
Even in the case of test subjects with injuries to the central receptor epithelium the same current density has a stimulating effect at all parts of the ganglion layer. Thus the familiar excitation patterns will emerge once more in this epithelium. For this reason flicker threshold minima must be set up for harmonious frequencies in the case of these patients as well.

In contrast to the ganglion epithelium of a healthy eye, which when electrically stimulated is innervated at every point equally by receptor impulse rates, in cases of impairment of the central receptor layer it only receives additional impulse rates from the undamaged cells of the receptor layer. In such a case the undamaged receptors occupy a ring-shaped area around the central defective portion. The impulses arising from the receptor cells and going on to the ganglion epithelium also innervate in the central area only a peripheral ring area. On the inner edge of this ring area the stimulation intensity increases with a bound. It is clear, that under such a condition the results are in favor of those excitation fields in the ganglion epithelium, which by themselves also exhibit at this edge the largest gradient of intensity. This means all those excitation patterns, for which some nodal ring lands on this inner edge or in whose proximity it comes to rest. Excitation patterns that do not satisfy this requirement are hindered also from standing out by the activity of the undamaged receptor area. Such fields alternate constantly with those of the type first described, as one goes up the scale of frequencies. This is shown in Fig. 35. We should then expect, that the tendential curve of the flicker threshold will no longer follow a monotonous ascending course but will appear on its part to modulate.

The records of test subjects H.E. and F.M. (Fig. 10a and c) clearly show this modulation. It is then understandable too, if the relationship described by equation 39, the relationship between excitation frequency and threshold voltage, is not fulfilled for this subject (see Fig. 36a and b).

In contrast to the above the injuries to the receptor epithelium are too

small for subjects R.I. and D.A. to produce deviations from the normal curve diagram of the threshold curve. As is shown in Fig. 37a and b, the pertinent diagrams are inconspicuous.



/72

Fig. 34 a-d. Voltage- f^2 diagrams of test subjects with totally impaired receptor epithelium

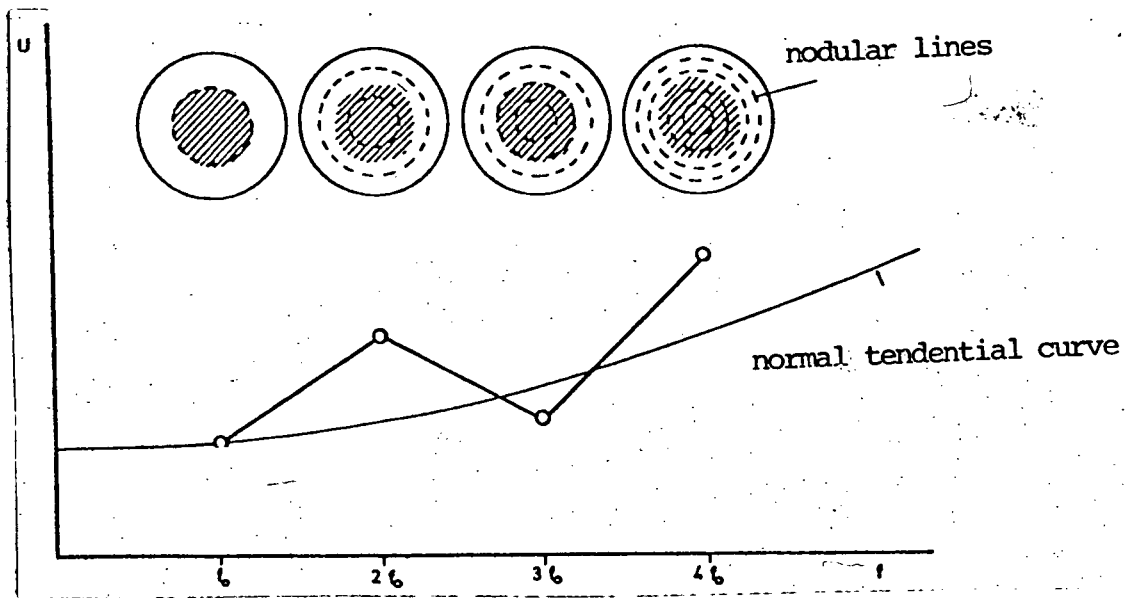
c) Injury to Global Ganglion Epithelium

/76

If the global ganglion epithelium is impaired, all interactions or its neurons will be destroyed. However we should not expect to find any minima of the flicker threshold according to the theory, since these neurons were held responsible for the appearance of excitation patterns and thus for the characteristic transfer behavior of the retina in respect to alternating stimuli. The flat curves, which we obtained from patients with total impairment of the central neural retina layers (Fig. 14 a-d), might correspond to a largely frequency independent excitation threshold of the optic nerve fibers.

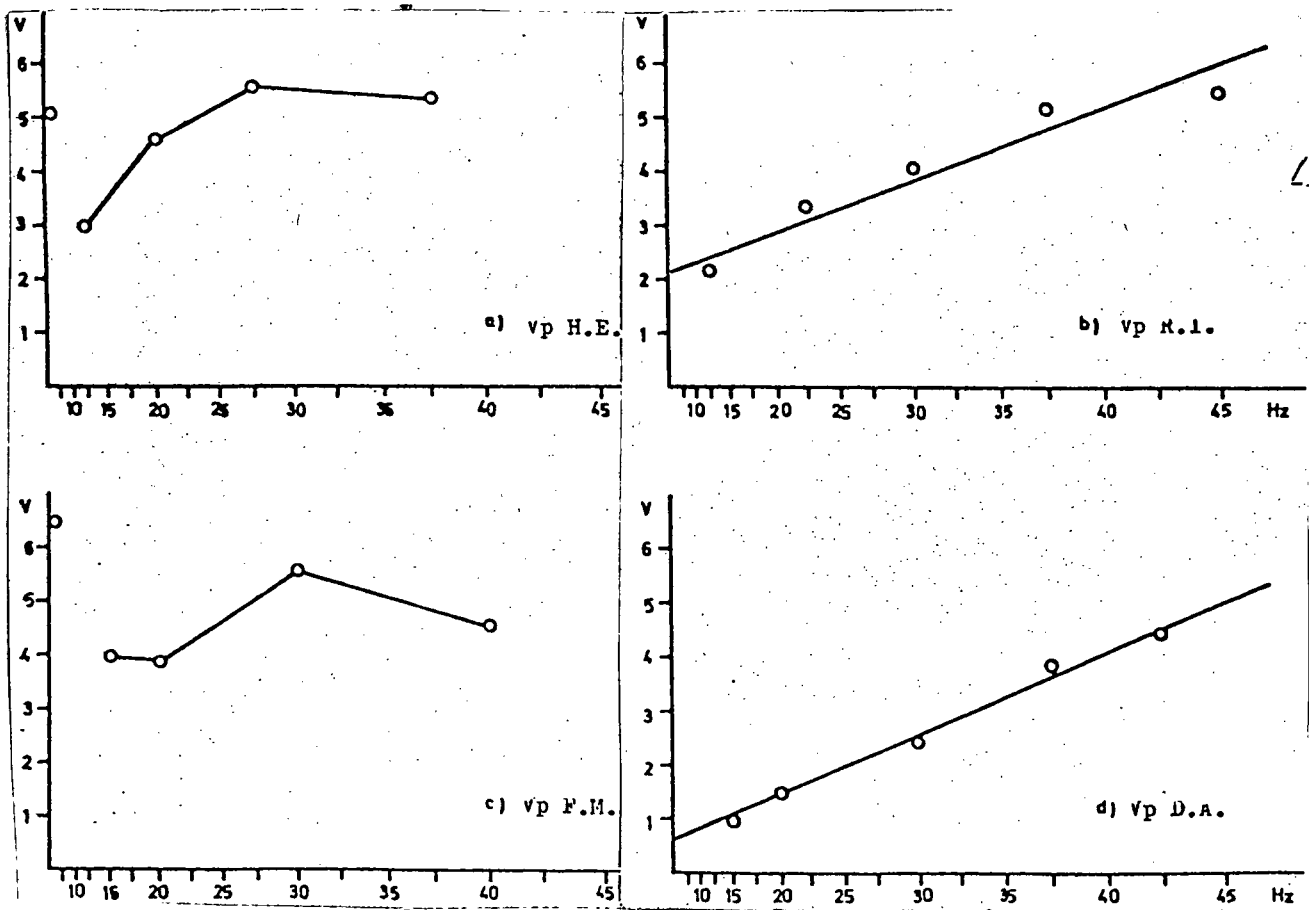
d) Injury to Central Areas of Ganglion Epithelium

In the experimental portion of this work it was shown, that injuries to



74

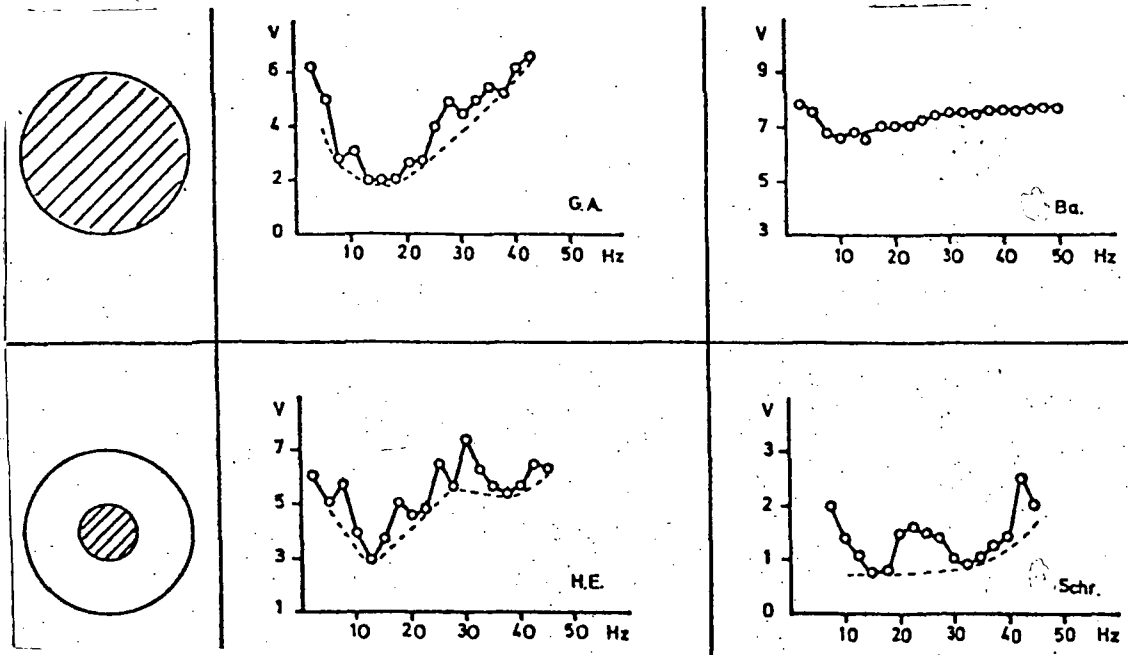
Fig. 35. Interpretation of modulated tendential curve for central injuries to the receptor epithelium (explanation in text).



75

Fig. 36 a-d. Voltage- f^2 diagrams for test subjects with injured central portions of the receptor epithelium

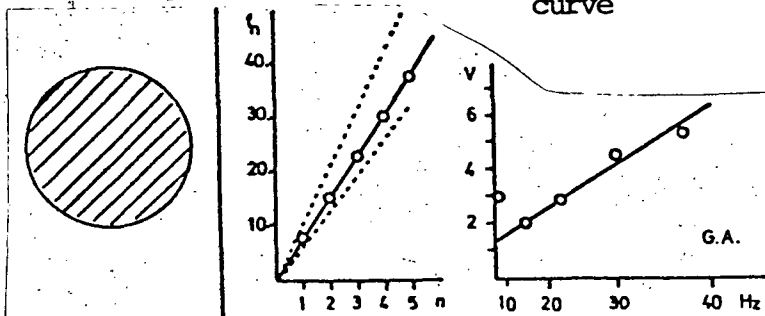
Receptor epithelium impaired Central neural retina layer impaired



/78

Fig. 38. Differentiation of retinal injuries based on flicker threshold curves

Injuries to receptor epithelium Injuries to central neural retina layers
 normal spectrum normal tendential curve



no test needed!

/79

normal spectrum abnormal tendential curve extended spectrum normal tendential curve

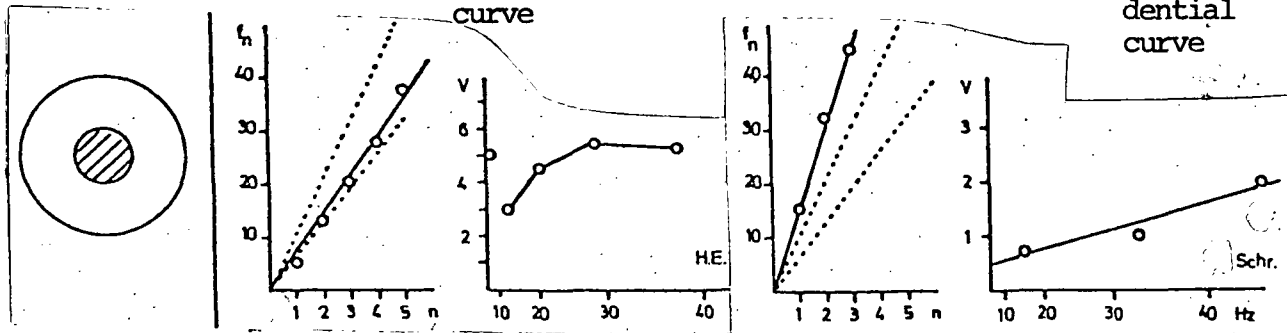


Fig. 39. Comparison of test nomograms for various injuries to the retina

the central area of the ganglion epithelium of course induce flicker threshold minima at harmonious stimulation frequencies but increase the value of the basic frequency to a point above the normal magnitude (8 Hz). Thus the flicker threshold curves for the corresponding patients seemed extended when compared with those of normal curve diagrams. This effect is easily explained by the proposed theory: because of the functional loss of central areas of the ganglion epithelium we must approximate the latter not by means of a circular disc but by a ring. The outer radius of this ring is in accord with the retina and the inner radius would be ΔR . In this ringlike ganglion epithelium, which we once more expose to a spatially homogeneous alternating excitation field, the excitation waves of the ganglion cells set up inbound and outbound concentric wave forms. However in this case the inbound waves are not reflected at the center of the epithelium but cophasically at its inner edge. We must therefore require, that an oscillation loop come to rest not only on the outer, natural edge but likewise on the inner edge (created by the area of degeneration). However this condition is met only by those waves, which conform to the reduced radius $R-\Delta R$ for the whole multiples of the half-waves. Together with the relationship (17) which always holds true, we have the appearance of the new excitation frequencies:

/77

(43)

$$f_n = \frac{c}{2(R-\Delta R)} \cdot n$$

Comparison with equation 19, which makes it possible to calculate the excitation frequencies of an undamaged ganglion epithelium, shows, that the basic frequency rises when there is impairment of the central areas of the ganglion layer.

Through these considerations we have made it basically possible to use the graph of the flicker threshold curve for differentiating pathological changes in the retina from a double point of view: one is that we can keep separate injuries to the receptor epithelium and those to the central neural layers; secondly we can keep apart total and partial (e.g. central) losses of one of the layers.

Representative examples are compared in the matrix diagram of Fig. 36. This matrix diagram is matched by another (Fig. 39), which contains those test diagrams which make it possible to test the harmony rule for minimum frequencies or the f_n^2 relationship for the tendential course (equation 39).

The experimental investigations on the electric excitability of damaged retinas make it possible, in combination with the theoretical interpretations which we have offered for the corresponding threshold curves in the last section, to hope for a simple procedure for differential diagnosis of retinal injuries. Such a procedure might be applied for example to patients with cataract diseases, where optical methods for examining the fundus are ruled out.

/80

REFERENCES *

11. Abe, Z., "Influence of adaptation on the strength-frequency curve of human eyes, as determined with electrically produced flickering phosphenes," Tohoku J. Exp. Med. 54, 37 (1951). /81
2. Brown, K.T. and T.N. Wiesel, "Intraretinal recording with micropipette electrodes in the intact cat eye," J. Physiol., 149, 537 (1959)
3. Brillouin, L., "Science and Information Theory," 2nd edition, Academic Press Inc., publishers, New York, 1963
4. Frank, H., "Informationspsychologie in Kybernetik, Brücke zwischen den Wissenschaften" [Information Psychology in Cybernetics, a Bridge between the Sciences], Umschau Verlag, Frankfurt a.M., 1965
5. Grüsser, O.J. and A. Grützner, "Neurophysiologische Grundlagen der periodischen Nachbildphasen nach kurzen Lichtblitzen," [Neurophysiological Bases for Periodic Afterphases following Short Light Flashes] v. Graefes, Archiv für Ophthalmologie 160, 65 (1958)
6. Hartline, H.K., "The response of single optic nerve fibers of the vertebrate eye to illumination of the retina," American J. Physiol. 121, 400 (1939)
7. Kuffler, S.W., "Discharge patterns and functional organization of mammalian retina," J. Neurophysiol. 16, 37 (1953)
8. Landois-Rosemann, "Lehrbuch der Physiologie des Menschen" [Textbook of Human Physiology], Volume 2, Verlag Urban & Schwarzenberg, Munich-Berlin, 1962
9. Motokawa, K. and K. Iwama, "Resonance in electrical stimulation of the eye," Tohoku J. Exp. Med. 53, 201 (1950)
10. Ogawa, T., P.O. Bishop and W.R. Levick, "Temporal characteristics of responses to photic stimulation by single ganglion cells in the unopened eye of the cat," J. Neurophysiol. 29, 1 (1966)
11. Polyak, S.L., "The Retina," U. Chicago Press, 1941
12. Shannon, C.E. and W. Weaver, "Mathematical Theory of Communication," U. Illinois Press, Urbana (J11) /82
13. Sneddon, I., "Spezielle Funktionen der mathematischen Physik (Formelsammlung II)" [Special Functions of Mathematical Physics (Formula Collection II)], B.I. Höchschultaschenbuch 54

ADDITIONAL LITERATURE NOT CITED IN THE TEXT

1. Knoll, M., "Anregung geometrischer Figuren und anderer subjektiver Licht-

* Tr. note: The original bibliography contains inaccuracies

- muster in elektrischen Feldern" [Excitation of geometrical figures and other subjective light patterns in electric fields], Schweiz. Zeitschrift für Psychologie und ihre Anwendung 17, 110 (1958)
2. Knoll, M. and J. Kugler, "Subjective light pattern spectroscopy in the electroencephalographic frequency range," Nature 148, 1823 (1959)
 3. Knoll, M., J. Kugler, J. Eichmeier and O. Höfer, "Note on the spectroscopy of subjective light patterns," J. Analyt. Psychol. 7, 55 (1962)
 4. Motokawa, K., "On the mechanism of periodic excitability of nervous tissue," Tohoku J. Exp. Med. 50, 307 (1949)
 5. Motokawa, K., and K. Iwama, "The electric excitability of the human eye as a sensitive indicator of oxygen deficiency," Tohoku J. Exp. Med. 50, 319 (1949)
 6. Motokawa, K. and K. Iwama, "The relation between the intensity of light and the electric excitability of the human retina," Tohoku J. of Exp. Med. 51, 155 (1949) /83
 7. Tukahara, S. and Z. Abe, "Resonance phenomena of photopic and scotopic receptors," Tohoku J. Exp. Med. 54, 189 (1951)
 8. Brown, J.E. and D. Major, "Cat retinal ganglion cell dendritic fields," Expl. Neurol. 15, 70 (1966)
 9. Leicester, J. and J. Stone, "Ganglion, amacrine and horizontal cells of the cat retina," Vision Res. 7, 695 (1967)
 10. Misotten, L., "The Ultrastructure of the Human Retina," Brussels (1965)
 11. Brown, K.T. and K. Tasaki, "Localisation of electrical activity in the cat eye by an electrode marking method," J. Physiol. 158, 281 (1961)
 12. Bornschein, H., "Der Einfluss zeitlicher Reizgradienten auf die Impulsaktivität retinaler Neurons der Katze," [Effect of Temporal Excitation Gradients on the Impulse Activity of Retinal Neurons in the Cat], Pflügers Arch. ges. Physiol. 275, 478 (1962)
 13. Granit, R., "Die Elektrophysiologie der Netzhaut und des Sehnerven (Mit besonderer Berücksichtigung der Flimmermethode)" [The Electrophysiology of the Retina and Optic Nerve (with special attention to the flicker method)], Acta Ophthalmologica, Copenhagen (1936)
 14. Graham, C.H. and R. Granit, "Comparative studies on the peripheral and central retina: inhibition, summation and synchronization of impulses in the retina," Amer. J. Physiol. 98, 664 (1931)
 15. Spinelli, D.H., "Receptive fields in the cat's retina," Science 152, 1768 (1966)
 16. Motokawa, K., "Periodic excitability of the human retina," Jap. J. of Physiol. 1, 16 (1950)